Development of a Cost Oriented Grinding Strategy and Prediction of Post Grind Roughness using Improved Grinder Models

Sriram Srinivasan

Thesis submitted to the faculty of the Virginia Polytechnic Institute and State University in partial fulfilment of the requirements for the degree of

Master of Science

In

Mechanical Engineering

John B Ferris, Chair
Saied Taheri
Corina Sandu

May 9th 2017
Blacksburg, Virginia

Keywords: Pavement Profiles, Diamond Grinding, Pavement Rehabilitation, Grinding Strategy, Genetic Algorithm Application

Development of a Cost Oriented Grinding Strategy and Prediction of Post Grind Roughness using Improved Grinder Models

Sriram Srinivasan

Abstract

Irregularities in pavement profiles that exceed standard thresholds are usually rectified using a Diamond Grinding Process. Diamond Grinding is a method of Concrete Pavement Rehabilitation that involves the use of grinding wheels mounted on a machine that scraps off the top surface of the pavement to smooth irregularities. Profile Analysis Software like ProVAL© offers simulation modules that allow users to investigate various grinding strategies and prepare a corrective action plan for the pavement. The major drawback with the current Smoothness Assurance Module© (SAM) in ProVAL© is that it provides numerous grind locations which are both redundant and not feasible in the field. This problem can be overcome by providing a constrained grinding model in which a cost function is minimized; the resulting grinding strategy satisfies requirements at the least possible cost. Another drawback with SAM exists in the built-in grinder models that do not factor in the effect of speed and depth of cut on the grinding head. High speeds or deep cuts will result in the grinding head riding out the cut and likely worsening the roughness. A constrained grinding strategy algorithm with grinder models that factor in speed and depth of cut that results in cost effective grinding with better prediction of post grind surfaces through simulation is developed in this work. The outcome of the developed algorithm is compared to ProVAL's© SAM results.

Development of a Cost Oriented Grinding Strategy and Prediction of Post Grind Roughness using Improved Grinder Models

Sriram Srinivasan

General Audience Abstract

Irregularities in road surfaces that exceed government standards are usually rectified using a Diamond Grinding Process. Diamond Grinding is a method of Concrete Pavement Rehabilitation that involves the use of grinding wheels mounted on a machine that scraps off the top surface of the pavement to smooth irregularities. The work aims to develop a computer program that can carry out simulations of the grinding process for engineers to use before actual grinding in the field. The developed program is then compared against industry standard simulators to obtain improvements.

.

Dedication

To my parents, my brother, my sister, and family for their continued belief and support

Acknowledgments

I would like to take this opportunity to thank my advisor, Dr. John B. Ferris for his support throughout my research. Right from early days at Virginia Tech, he always had time to provide me with both academic and research assistance. Dr. Ferris was instrumental in pointing me in the right direction in organizing the theory, concepts and code for my research. I would also like to thank Dr. Taheri & Dr. Sandu for their support.

A special thanks to the people at Surface Systems & Instruments (SSI) for sponsoring my research and to Nicholas Schaefer for his support in clarifying my queries regarding the technical aspect of my research.

I would also like to extend my gratitude to the Vehicle Terrain Performance Laboratory for allowing me the opportunity to work. I would also like to appreciate the support extended by my friends and students within the lab.

Finally, I would like to thank my family for their motivation and support throughout my graduate study. None of this would have been possible if not for their continued belief in me that had been the main force propelling me towards completing my degree.

Table of Contents

List of Figures

List of Tables

Nomenclature

IRI	International Roughness Index
h_p	Profile elevation
h_{ps}	Smoothed Profile Elevation
L_p	Moving average filter base length
Δ	Sample interval
T	Time for Simulation to travel over profile
L	Length of the Profile
$\lvert\dot{z}\rvert$	Suspension Velocity Magnitude
k_t	Tire Stiffness
k_s	Spring Stiffness
m_u	Unsprung Mass
m_s	Sprung Mass
c_s	Spring Damping Coefficient
x_s	Sprung mass displacement
x_u	Unsprung mass displacement
z_r	Road Elevation
$\dot{x_s}$	Sprung mass velocity
$\dot{x_u}$	Unsprung mass velocity
s_{ps}	Smoothed Elevation slope
X_{f1}	Location of front tandem wheel 1 – Longitudinally
X_{f2}	Location of front tandem wheel 2 – Longitudinally
X_{r1}	Location of rear tandem wheel 2 – Longitudinally
X_{r2}	Location of read tandem wheel 2 – Longitudinally
X	Location of grinder head – Longitudinally
L_r	Distance between Grinding head and Front Tandem Wheels
L_r	Distance between Grinding head and Rear Tandem Wheels
$P(X)$	Original Profile Elevation with respect to longitudinal Distance
$G(X)$	Grinded Profile Elevation with respect to longitudinal Distance
H_f	Average elevation of front tandem wheels

H_r	Average elevation of rear tandem wheels
H_{ref}	Height of the grinder reference frame at start location
H_{grind}	Height of the grinder reference frame at grind location
H_{head}	Height of the grinding head from the profile height at start location
α	Angle of Attack between Cutting Head and Ground
δ	Depth of Cut
R	Radius of Cutting Head
v	Velocity of Grinder advancing along the road surface

1. Introduction

The need for smooth roads has been the pursuit of contractors and Highway Authorities for many years. The benefits of smooth roads to ride, comfort and safety of the users are well documented. Smooth roads are also beneficial to highway construction and maintenance contractors due to possible incentives from local Department of Transportation's (DOT) and Federal Highway Administration (FHWA). Islam and Buttlar calculated that a vehicle user will spend $349/year more when driving on a road of International Roughness Index (IRI) 200in/mi compared to an IRI of 110in/mi [1]. The American Association of State Highway and Transportation Officials (AASHTO) estimated in 2009 that 76.8 billion US dollars are spent annually on poor road conditions in the country [2]. Road roughness is inherent in all road profiles, both new and old. Road surfaces gradually undergo deterioration and damage over the years due to wear & tear, weather, traffic flow and other detrimental factors. These result in an increase in road roughness that needs to corrected. The 21st Annual Highway Report on State Highways shows that on average $26,079 are spent on maintenance disbursements per mile of highway. The report also states that the year 2012 saw a total of 20.8 billion US dollars were spent on maintenance related activities across the nation [3].

Road Roughness data are generated by measuring longitudinal profile data and converting them to roughness statistics through mathematical analyses [4]. The commonly utilized measurement is the International Roughness Index (IRI). The IRI concept involves the measurement of roughness based on vehicle suspension travel over distance traversed. Another form of roughness are localized roughness events such as slab potholes, slab distortions, Faults, Curling and Breaks [5]. FHWA and State DOT's require contractors to meet both localized roughness limits and overall roughness measures such as IRI thresholds while constructing new pavements or maintaining existing pavements.

Pavement rehabilitation is a technique used to correct localized roughness events and also to bring the overall IRI over the length of the road within specifications. Concrete Pavement Rehabilitation (CPR) is a subset that is utilized to correct concrete streets, highways and airports. CPR is a viable economical alternative to asphalt overlay and the benefits of CPR are numerous [6]. CPR techniques have proven to be long lasting, simple, environmentally friendly and cost effective.

Some common CPR techniques that are utilized widely are Stab Stabilization/Jacking, Partial Depth Repair, Cross Stitching, Dowel Bar Retrofit, Full Depth Repair, Diamond Grinding, Diamond Grooving and Joint & Crack Resealing [7]. These techniques need to be used in combinations based on the requirement of the job, desired result and extent of damage to the existing pavement. Figure 1 [8] plots the rate of deterioration in the condition of the pavement against years of operation or traffic flow. It also shows the windows of opportunity along the life cycle of the pavement where different CPR techniques can be used by maintenance contractors.

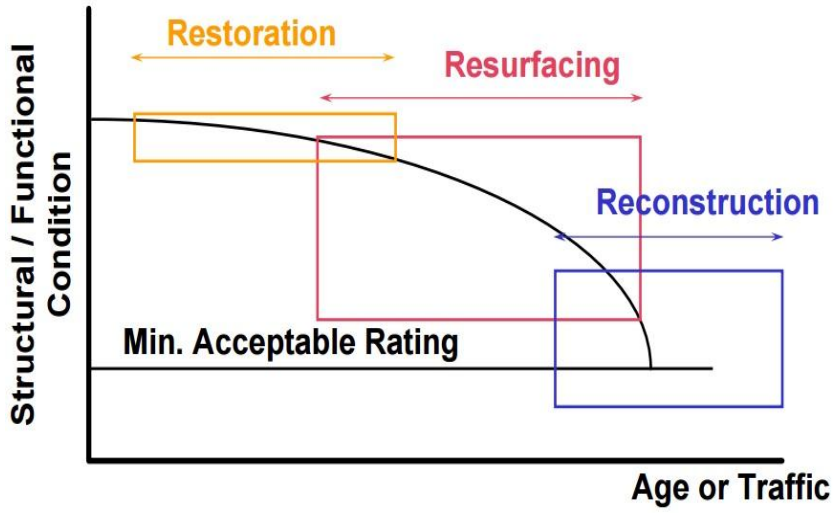

Figure 1: Timeline for Various Pavement Correction [8]

Diamond Grinding is a commonly applied CPR technique used to correct roughness events. Diamond grinding is defined as the removal of a thin layer of concrete top surface to restore smoothness and friction. Diamond grinding has been employed as a method to improve road surfaces since 1956 and produces improvements in roughness index, skid resistance, increased surface macro texture and reduction in pavement noise [9] . Diamond grinding is a viable method to improve surface roughness of pavements that is both cost effective and comparatively easy with respect to other methods of rehabilitation.

1.1 Motivation for research

The major problem faced by highway contractors and engineers is to predict the resultant road profiles corresponding to various grinder settings. The need to identify locations to grind and the grinder settings at these locations is paramount for determining a grinder strategy. One method to carry out these “what-if” analyses is to use Profile Analysis

Software like ProVAL©'s Smoothness Assurance Modules to determine a grinding strategy. This software uses 2D grinding simulations to predict post grind surfaces based on inbuilt grinder models. The use of these algorithms has become standard practice in the pavement industry but their accuracy in predicting post grind surface is limited due to an overly simplified grinder model. [10].

One of the available commercial grinding simulation on the SAM module of ProVAL© is outlined in [11]. One inherent drawback with this software is the absence of a constraint model in identifying grinding locations. This can result in unrealistic or redundant grinding locations. Moreover, the associated cost plays a huge role in making grind/no grind decisions for engineers but is omitted in these algorithms. The other shortcoming in commercially available code is the implementation of rigid grinder models. The grinders are characteristically complaint and naturally deflect when interacting with the pavement. This will change the grinding results which is currently overlooked. The major differences between real world grinding and commercial grinding simulators are summarized in Table 1.

Table 1: Difference between real world grinding & grinding simulators

Real World Grinding	**Grinding Simulators**
Grind / No grind decisions based on cost benefits as well as IRI thresholds	Grind / No grind decisions based solely on IRI thresholds
Grind locations identified based on machine capabilities (i.e. Grind locations placed too close together are combined rather than rising grinding head and lowering again)	No constraints considered. The algorithm might result in unrealistic grinding locations.
Speed of grinding and depth of cut determine post grind surface	Speed of grinding and depth of cut are not considered during the simulation

1.2 Problem Statement

The primary objective of the research is to develop a grinding simulator that resolves the ambiguity in the grinding process by incorporating a constraint model in which the user can provide constraints to limit cost, amount of grinding etc. A strategy is developed to bring road surfaces within roughness specification without over grinding and at a minimum cost.

This is achieved by the development of a cost function that will optimize the grinding strategy to achieve the desired IRI improvement while incurring lower costs. Secondly, the algorithm will incorporate compliant grinder models that include speed and depth of cut in predicting post grind surface. The results are compared to the commercially available grinding simulators and conclusions on the improvement are drawn based on the results.

1.3 Thesis Statement

Results of the concrete grinding process can be more accurately predicted with the development of compliant grinder models and these improved predictions can be implemented in a cost analysis framework that maximizes the value of the grinding process.

1.4 Main Contributions

The major contributions of this work are summarized hereby.

- A grinding simulator to run "what-if" analyses prior to diamond grinding on actual pavements including a constrained cost function to minimize costs.
- Linear Cost function to calculate the cost associate with grinding a stretch of pavement.
- A Compliant grinder model that includes the speed of operation and depth of cut to calculate amount of material removed.

1.5 Publications

The research was presented in the following conference.

- *28th Annual Road Profile User's Group Conference*, San Diego on November 3rd 2016.

1.6 Thesis Outline

The remainder of this document is laid out as follows. First, a brief background on Roughness measurement, the Diamond Grinding process, and 2D Grinding Simulators is presented. Next, a novel grinding strategy is developed including the various costs associated with the process and the operational constraints. Following that, the modelling of the complaint grinder model is developed. The effect of speed and depth of cut on the grinding

head is elucidated and modelled. These grinder models and cost function are then combined into a grinding simulator algorithm to develop grinding strategies. A discussion on the simulator and future work follows.

2. Background

2.1 Pavement Profiles and Road Roughness

Pavement profiles are a sequence of height measurements of the road surface along a longitudinal path that can be then utilized to analyse and classify the road surface. Different profiles of the same road surface can be taken by collecting data along different paths. Longitudinal profiles are utilized to calculate roughness of the surface [12]. The earliest systems collected data using instrumented vehicles known as "Response Type Road Roughness Measuring Systems" (RTRRMS). Roughness measurements from such equipment are typically normalized over the longitudinal distance traversed. This results in measures of slope in the units of inches per mile or meters per kilometre [4].

Pavement profilers usually compute the profile from three distinct measurements. Profilers combine a reference elevation, height relative to the reference and longitudinal distance to estimate the true pavement elevation. Figure 2 shows the schematic of a typical inertial profiler system where the grey line shows the inertial reference height (reference elevation), A non-contact transducer like a laser is used to measure the relative reference to the ground. The data from the accelerometers are used to compute an inertial reference for the height of the accelerometers and the vehicles speedometers provide the longitudinal distance. These three elements are then combined to provide the longitudinal road profile. In 1960, GM designed the inertial profiler to perform high speed profiling of pavement surfaces, a major breakthrough in the field of pavement profiling [12]. Figure 3 shows a present day inertial profiler with front mounted lasers. These commercial profilers are widely used at highway speeds for profiling road surfaces and calculating road roughness.

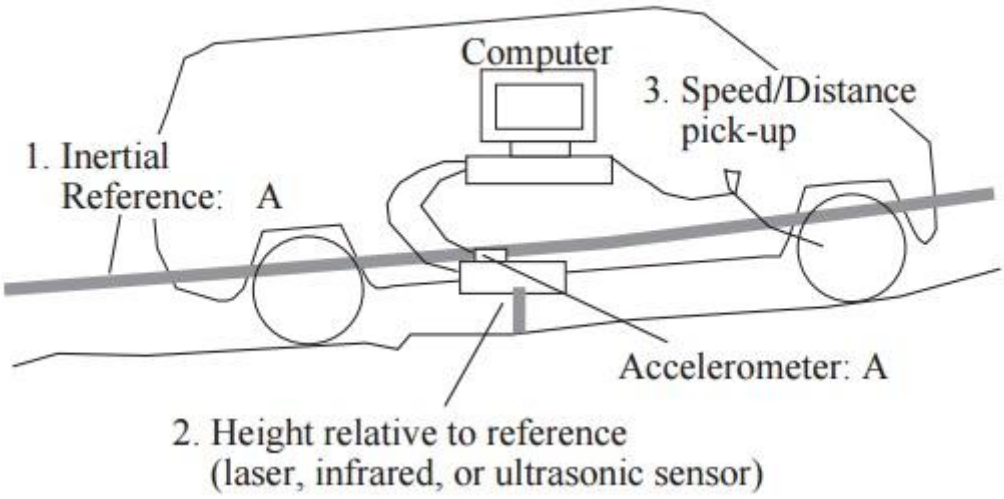

Figure 2: Inertial Profilers

Figure 3: Current Commercial High Speed Profilers

Figure 4 shows a typical elevation profile that results from data collected using inertial profilers. They include the heights measured by the lasers plotted against the longitudinal distance travelled by the profilers. These elevation profiles are then converted into roughness measures using mathematical analyses to characterize the terrain.

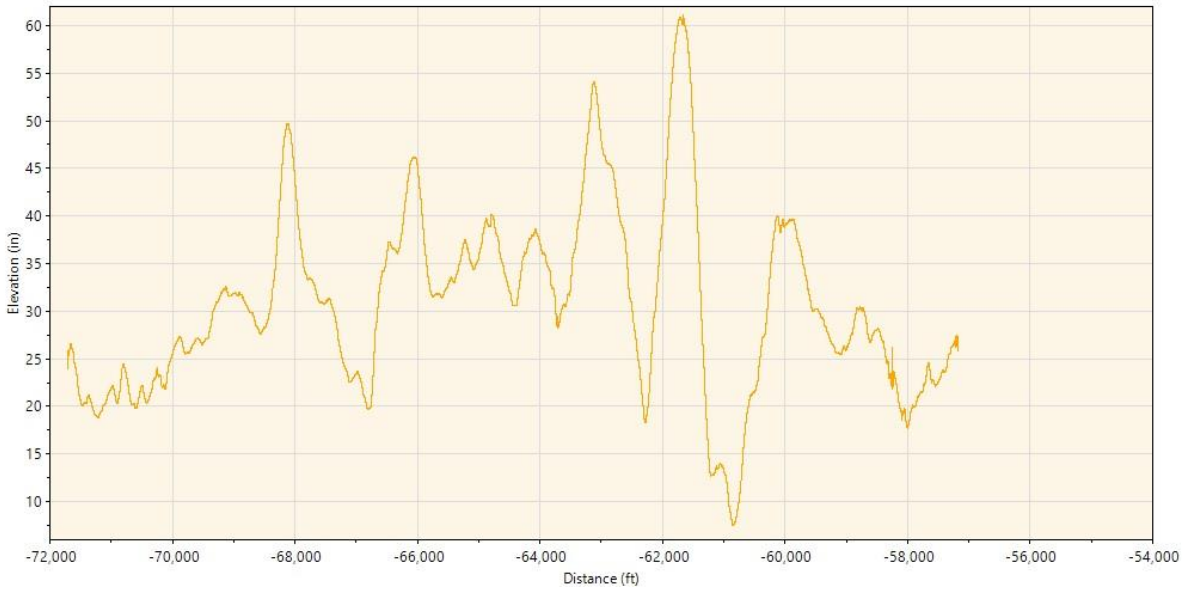

Figure 4: Sample Elevation Profile

The Profilograph Index (PrI) and the International Roughness Index (IRI) are the most commonly used roughness indices in the United States. Terrain Roughness measurements are essential for a wide range of industries. Pavement engineers nationwide use these data for identifying when to maintain or relay road surface across the country. Vehicle engineers utilize them to perform simulations of vehicle durability. Federal Highway Administration utilizes these Roughness measurements on its Highway Performance Monitoring System (HPMS) that contains data on all highways across the United States. Each year, every state is required to report their IRI values for all highways that will then be updated in the HPMS system for monitoring and maintenance activities [14].

The International Roughness Index (IRI) was originally developed by the World Bank as part of the International Road Roughness Experiment (IRRE) held in Brazil in 1982 [15]. The IRI is the standard roughness reporting standard due to its reproducibility among different types of equipment including singe and two track profiling, Rod & Level and RTRRMS. The National Cooperative Highway Research Program (NCHRP) carried out research to develop a computer algorithm to calibrate the RTRRMS type profile equipment. This research led to the develop of a particular set of parameters called as the "Golden Quarter Car" Parameters. These parameters are utilized in the calculation of the IRI and resulted in "Virtual response type system" [12].

The International Roughness Index is a scale for roughness based on the simulated response of a generic motor vehicle to the roughness in a single wheel path of the road

surface. The IRI is determined by obtaining a suitably accurate measurement of the road profile, processing it through an algorithm that simulates the way a reference vehicle would respond to the inputs and accumulating the suspension travel. In order words, it's the accumulation of the absolute suspension travel obtained by simulating the Golden Quarter Car travelling at 80 kph over the single wheel track and normalized it over the distance travelled (1).

$$IRI = \frac{1}{L}\int_0^T |\dot{z}|dt \tag{1}$$

The variable $|\dot{z}|$ represents the magnitude of the suspension velocity (the difference in velocity between the sprung and unsprung masses), the result of the integral is the accumulation of the suspension travel over the entire duration of the simulation. The accumulated suspension travel is then normalized over the distance of the road segment, L to obtain the IRI for the particular segment. The IRI values are typically between 1 to 2 m/km for superhighways, 2.5-3 m/km for newly laid pavement and between 2.5 to 5 m/km for older pavements [12]. The lower number of IRI indicates smoother roads that progressively become rougher with increase in IRI. Typically, unpaved surfaces have an IRI above 5 m/km.

The IRI can be calculated from the longitudinal road profile by utilizing a Linear Time Invariant filter to simulate the quarter car parameters. [16] [17]. This methodology involves first filtering the road profile over a 250mm moving average filter. This filter is required to simulate the effect of tire enveloping over surface irregularities and cracks. This mimics the physical behaviour of tires in reducing sharp wavelength excitations when running the quarter car simulations with a point-follower ground contact model. This is followed by the quarter car simulation to calculate and accumulate the suspension travel over the length of the profile. The IRI equals the difference between the accumulated suspension response between the sprung and unsprung mass (z_s, z_u). Figure 5 schematically shows the simulation setup of the quarter car model. z_r is the filtered road profile, z_u & z_s are the changes in elevation of the sprung mass and unsprung mass due to the road profile. The values of $m_s, m_u, k_s, k_t and\ c_s$ are provided by the golden quarter parameters. These parameters were chosen to replicate the typical passenger car and hence make the IRI representative of what is actually experienced by road users. The parameters are scaled according to the sprung mass m_s of the vehicle to make the measure applicable to a wide range of vehicles. The IRI golden quarter car parameters are given in Table 2 [18] [19].

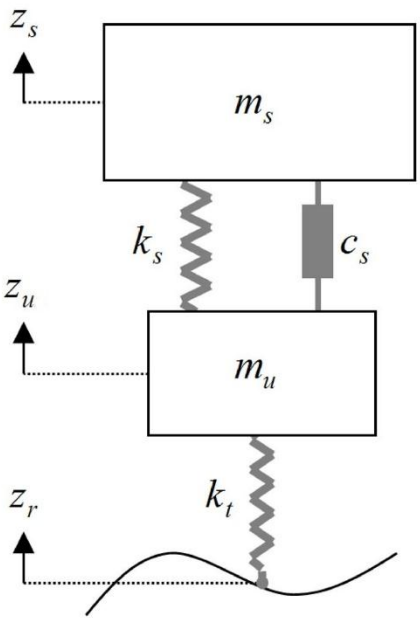

Figure 5: Schematic of Quarter Car Simulation

Table 2:Golden Quarter Car Parameters Normalized by Sprung Mass

Parameter	**Value**
Spring Stiffness, K_s	$63.3m_s$
Tire Stiffness, K_t	$653m_s$
Suspension Damping, C_s	$6m_s$
Unsprung Mass, m_u	$0.15m_s$

The IRI can be made sensitive or non–sensitive to excitations by the base length of the moving average filter prior to the quarter car simulation. That is, roughness events can be hidden or exaggerated based on the filter. The users have the discretion to choose an appropriate wavelength based on their own points of interest. Shorter base length will make the IRI higher while increasing the base length will make the profile smoother. This is because a higher base length will remove some of the roughness events from the actual road profile. The State Department of Transportation and FHWA usually specify two types of IRI specification for paved road surfaces in the United States. A longer wavelength of 528ft is utilized to specify the Long- Continuous IRI while a shorter wavelength of 25ft is used to

identify locations of localized roughness also known as Short – continuous IRI. Hence, for contractors to get paid on a project, they need to meet both the specifications or, in some cases, either one based on the state.

2.1.1 Calculating IRI from Road Profile

A standard step by step method for calculating the IRI is described in the following section. [16] [17]. The primary input for calculating the IRI is a road elevation profile sampled at an interval of 300mm or less. The need for this sampling interval is due to the method of interpolation used in the algorithm. The International Road Roughness Experiment (IRRE) conducted a study on the different types of interpolation techniques and their accuracy with IRI measurements and concluded on utilizing a linear interpolation with constant slope. It was shown by Sayers [16] that linear interpolation has low accuracy at sampling intervals of 300mm or higher. The first step in the process is to run a 250mm moving average filter to smooth out the data. The is carried out using the following equation.

$$h_{ps}(i) = \frac{1}{k} \sum_{j=i}^{i+k-1} h_p(i) \tag{2}$$

$$k = \max[1, \frac{L_p}{\Delta}] \tag{3}$$

The ASTM calculation of the IRI involves the utilization of the Linear Time Invariant (LTI) filter to simulate the quarter car over the road profile. The system expressed in state space form is as given below:

$$\dot{x} = Ax + Bu \tag{4}$$

$$y = Cx + Du \tag{5}$$

The state space equation in (4), (5) can be written in matrix form using the golden quarter car parameters are follows

$$\begin{vmatrix} \dot{x}_! \\ \dot{x}_2 \\ \dot{x}_3 \\ \dot{x}_4 \end{vmatrix} = \begin{bmatrix} 0 & 1 & 0 & 0 \\ -k_s/m_s & -c_s/m_s & k_s/m_s & c_s/m_s \\ 0 & 0 & 0 & 1 \\ k_s/m_u & c_s/m_u & -(k_t+k_s)/m_u & -c_s/m_u \end{bmatrix} \begin{vmatrix} x_s \\ \dot{x}_s \\ x_u \\ \dot{x}_u \end{vmatrix} + \begin{vmatrix} 0 \\ 0 \\ 0 \\ k_t/m_u \end{vmatrix} h_{ps} \quad (6)$$

$$y = |-1 \quad 0 \quad 1 \quad 0| \begin{vmatrix} x_s \\ \dot{x}_s \\ x_u \\ \dot{x}_u \end{vmatrix} + [0]h_{ps} \quad (7)$$

The above equation is used to solve for the state variable from which we can calculate the location of the sprung and unsprung masses over the entire length of the profile.

$$IRI = \frac{1}{L}\int_0^{L/V} |\dot{x}_s - \dot{x}_u|\, dt \quad (8)$$

But, to solve the linear equation in (6), we use the matrix exponential, Sayers [17] suggests that the total response at the $'i^{th'}$ location is equal to the free response up to the point $'i-1'$ plus the forced response between the interval $'i-1' and 'i'$. The closed form solution can be given by the following equation where Δ is the sampling interval, V the golden quarter car simulation velocity of 80 kmph.

$$x_i = e^{\frac{A\Delta}{V}} x_{i-1} + A^{-1}\left(e^{\frac{A\Delta}{V}} - I\right)Bu \quad (9)$$

Using the assumption of linear interpolation and constant slope between data points, the input in (9) can be substituted as the slope between interval $'i-1' and 'i'$, we can estimate the state along the road profile (10). Replacing the input in (9) with slope will change the states of the linear state space model as shown in (11)

$$x_i = e^{\frac{A\Delta}{V}} x_{i-1} + A^{-1}\left(e^{\frac{A\Delta}{V}} - I\right)Bs_{ps} \quad (10)$$

$$\boldsymbol{X} = |s_s \quad \dot{s_s} \quad s_u \quad \dot{s_u}| \quad (11)$$

The IRI can then be calculated using the new accumulator as defined below.

$$\boldsymbol{IRI} = \frac{1}{n}\sum_{i=i}^{n}\left|s_{s_i} - s_{u_i}\right| = \frac{1}{n}\sum_{i=i}^{n}|CX| \tag{12}$$

To initialize the algorithm Sayers recommends, based on a computer study that minimizes error, that the initial $z_s \; and \; z_u$ should be set to match the height of the first profile points and $\dot{z_s} \; and \; \dot{z_u}$ should be set to match the average change in profile height per second over the first 11m of the profile (13).

$$x_1 = \left| \frac{h_{p\frac{11}{\Delta}} - h_{p_1}}{11} \quad 0 \quad \frac{h_{p\frac{11}{\Delta}} - h_{p_1}}{11} \quad 0 \right| \tag{13}$$

2.2 Mean Roughness Index (MRI)

Another index of interest with respect to the Diamond Grinding Process is the Mean Roughness Index (MRI). The MRI utilizes both wheel tracks instead of a single wheel track when computing the roughness. The IRI is computed for each wheel track separately and averaged along the entire profile to obtain the MRI [12].

The diamond grinding process is based only on the IRI and MRI specifications. but, other roughness indices also exist. A detailed review of each index is compiled by Alvarez and not reproduced here [14].

- Profilogragh Index (PrI)
- Spectrum Evenness Index (SEI)
- Truck Ride Index (TRI)
- Longitudinal Evenness Index (LWI)
- Pavement Quality Index (PQI)
- Vehicle Response Index (VRI)
- The Corrected Unevenness Index (C_w)
- Ride Quality Index (RQI)
- Health Index (HI)
- Ride Condition Rating (RCR)
- Full-Car Roughness Index (FRI)
- Roughness Index for Driving Expenditure (RIDE)
- Half Car Roughness Index (HRI)

- Mean Roughness Index (MRI)
- Dynamic Load Index (DLI)
- Heavy Articulated Truck Index (HATI)

2.3 Overview of Pavement Rehabilitation Techniques

Concrete and asphalt pavements all across the country are under constant wear and tear due to exposure to vehicles, weather, soil degradation and other detrimental effects. Pavement Rehabilitation is a broad name given to various activities carried out by state DOT's to fix roads that are rougher and are in need of maintenance. Identifying public roads that require rehabilitation is one of the most important outcomes from the HPMS program of highway monitoring. There are numerous ways for carrying out the process including Full Depth Repairs, Crack Resealing, Cross Stitching, Diamond Grinding, Grooving, Asphalt overlay, Cold Milling, and many more [7] [20]. This poses an interesting problem for selecting the appropriate method. The selection is usually made on a given set of constraints including required service life, nature of rehabilitation, costs of the operation and estimated life cycle costs in the future [7] [21].

Rehabilitation techniques are broadly classified into three categories based on the problems they address and when they are carried out along the service life of a pavement. They are [7]:

- Preventive Techniques: Proactive methods carried out prior to any signs of damage or deterioration. They slow down decline in pavement quality.
- Corrective Techniques: Reactive methods that are used to address specific problems in pavement quality and are only effect in corrective those.
- Corrective & Preventive Techniques: Carried out alternatively as both preventive measures and corrective actions based on the project requirements.

A brief description of some of the common rehabilitation techniques and their benefits are provided in the following sections.

2.3.1 Dowel Bar Retrofit

Dowel bar retrofit is a corrective and preventive CPR techniques that is aimed at increasing load transfer efficiency of joints in both plain and reinforced concrete [7]. Steel dowel bars are inserted across joints/cracks to reinforce the pavement. It is typically used to address faulting and cracks. Figure 6 shows how the process is carried out by cutting three grooves in each path across the cracks that need reinforcement. Following that, epoxy coating dowel bars are inserted into the slots as shown in Figure 7 and the slots are filled and finished to required smoothness. A dowel bar retrofit carried out during the laying of new pavement will be considered a preventive technique while one carried to address an increase of cracks of an existing pavement will be a corrective measure.

Figure 6: Slots along each wheel path

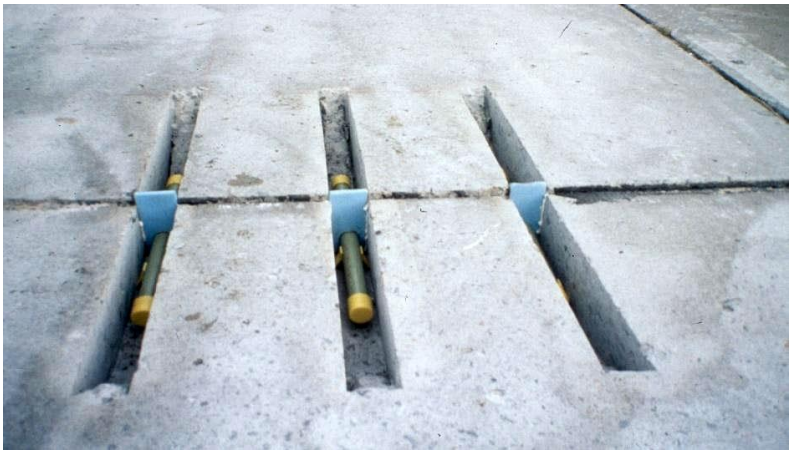

Figure 7: Dowel Bars inserted into Slots

2.3.2 Full Depth & Partial Depth Repairs

Full depth and partial depth repairs (FDR's and PDR's) are corrective rehabilitation techniques that are used to increase the service life of existing pavement. Depth repairs usually involve the replacement of an entire slab or portions of it to correct faulting and cracking in them. Figure 8 shows the three distinct steps in depth repairs. The process starts with identifying slabs that need repairs, then the slab is removed is either entirely or partially using saw cutters and finally re-laid fresh. Figure 9 shows how saw cutters are used to remove the slab without any damage to the adjoining slabs along the surface. The process is fast, easy and relatively inexpensive while compared to other techniques [7]. Partial Depth repairs involves removing up to 1/3rd of the slab.

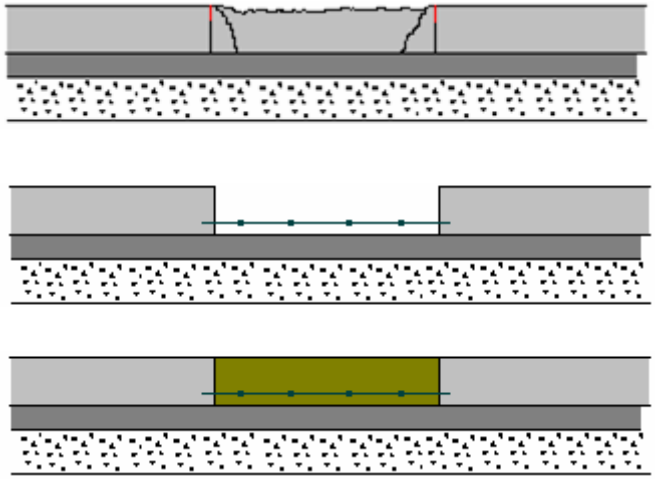

Figure 8: Full Depth Repairs – Schematic

Figure 9: Removing slab for replacement

2.3.3 Slab Stabilization

Slab Stabilization is both a preventive and corrective method. It is a technique that is used to increase stability from subgrade to the slab by filling voids and vacuums. The voids occur beneath the slabs due to usage and surface water infiltration. The resulting reducing of support will result in cracking and loss of structural integrity of the pavement. The process is usually carried out by pumping a type of foam or grout through holes drilled into the slab at locations of faulting. The green arrows in Figure 10 shows the development of cracks in the pavement due to the downward force of traffic due to voids in the substrate. The upward arrows in Figure 11 shows the generation of restorative force due to the injection ofgrout or form into the substrate. After this process, downward forces due to traffic are balanced by the reactive forces of the substrate. Further faulting or crack propagation is prevented by this method

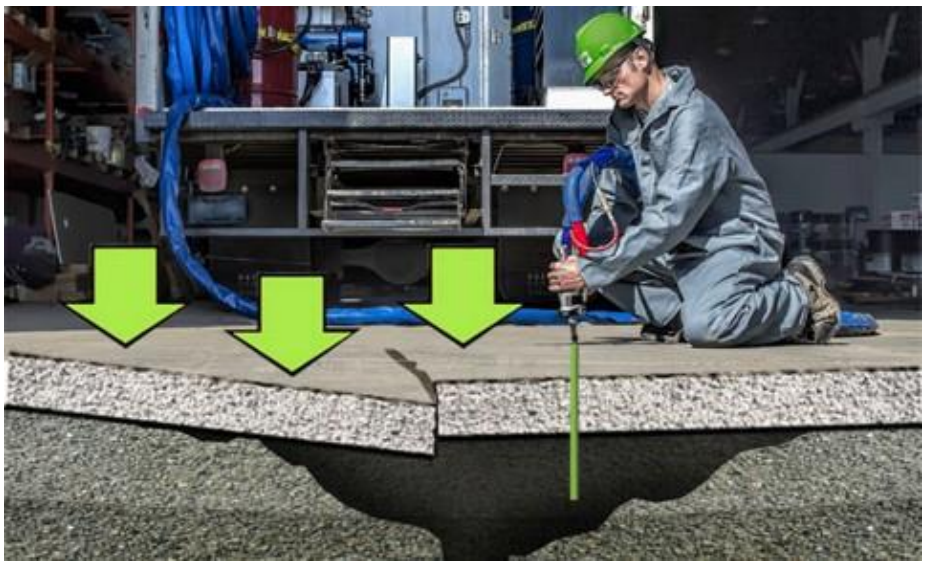

Figure 10: Voids beneath concrete pavement

Figure 11: Voids filled with Foam or Grout

2.3.4 Asphalt Overlay

The method of Asphalt overlay is used for both concrete and asphalt pavements. As the name suggests, it involves overlaying the damaged pavement with a thin layer of asphalt to reduce roughness and deformations in the pavement. It usually involves a thin course of about 1.5” to 2” of asphalt over the existing surface [22]. Figure 12 shows a thin edge of an asphalt overlay with a fog line painted. This hides any imperfections or faulting present in the base surface when calculating roughness.

Figure 12: Asphalt Overlay over existing pavement

2.3.5 Cold Milling

The method is exclusively used in asphalt pavements. It involves the use of a cold milling machine which is fitted with carbide tipped cutting drum that removes a thin layer of the top surface. This is results in improved surface texture and slid resistance. Cold milling is also used to correct imperfections and surface finishing of laid pavements. The milling machine typically operates along with dump trucks that collects the cut material as shown in Figure 13. The removed material is usually recycled for future use.

Figure 13: Cold Milling of Asphalt pavement

2.3.6 Cold In-Place Recycling

Cold in Place (CIR) Recycling is a method of rehabilitating damaged asphalt pavements by recycling the existing pavement and relaying the same again. The process is carried by using an assembly line of equipment working together to recycle the pavement. The process involves the following steps and equipment [23].

- Cold Milling to cut and remove the existing pavement.
- Crushing machine to crush the removed materials to required gradation.
- Mixing equipment to mix the crushed materials with binders to produce recycled asphalt.
- Asphalt pavers to lay the recycled material.
- Compaction equipment to finish the pavement for usage.

The process is economical and environment since materials from the existing pavement are reused rather than laying a new course to correct the pavement. Cold In-Place Recycling requires a train of equipment. The process starts with a milling machine that removes the existing pavement, a crusher to grind the pavement, a pugmill to mix the contents with additives and a paver to re-lay the pavement. These equipment as connected in a train as shown in Figure 14.

Figure 14: Cold Recycling Equipment on site

2.4 Overview of Diamond Grinding Operation

Diamond grinding is a preventive and corrective measure for concrete pavement rehabilitation. It involves the utilization of diamond saw blades to grind concrete pavements. The process involves stacking up diamond saw blades on shafts. The blades are spaced about 160 to 195 blades per meter based on the required texture and surface properties. The system is attached a water cooling system and the entire assembly is mounted under a machine to plane and level concrete. A vacuum system is incorporated to remove the material after grinding [24].

2.4.1 Early Usage of Diamond Grinding

The first version of today's diamond grinder was invented and build by Cecil W. Hatcher in the year 1962 which he christened as "The Bump Cutter" [25]. The invention describes a self-propelled machine with cutting wheels for removing bumps from concrete pavements. These early bump cutters where used in removing bumps from airport runways, roads and like.

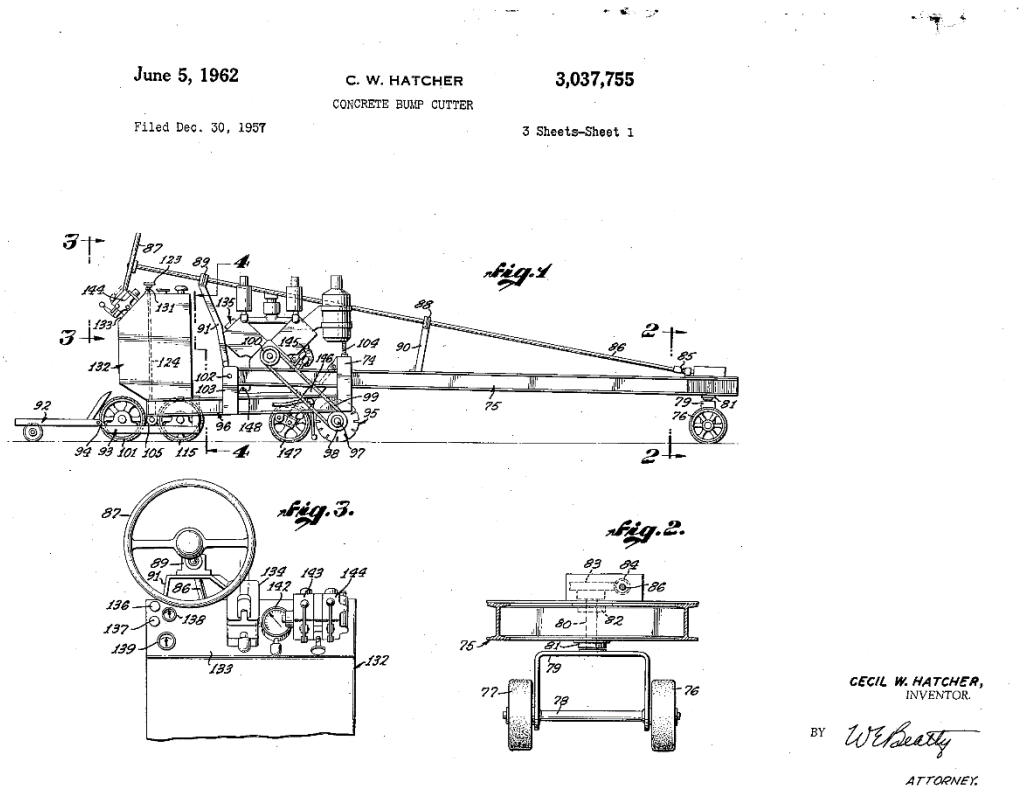
June 5, 1962 C. W. HATCHER 3,037,755
CONCRETE BUMP CUTTER
Filed Dec. 30, 1957 3 Sheets-Sheet 1
Fig. 1
Fig. 3.
Fig. 2.
CECIL W. HATCHER, INVENTOR.
BY W. E. Beatty
ATTORNEY.

Figure 15: Bump Cutter - 1962

These bump cutters where used for highway rehabilitation for the first time in 1965 when they were considered for a project by the California Department of Transportation as an alternative for asphalt overlays [24]. Since then Caltrans has been one of the pioneers in using Diamond Grinding for maintaining old and worn out pavements using Diamond Grinding.

2.4.2 Diamond Grinding - Parameters

Diamond grinding typically involves grinding 3/16" to 1/4" (5 to 7 mm) of the concrete pavement to smooth and level out the pavement. The process results in a grooved and textured surface that results in improved pavement performance and safety. The corduroy

texture also results in noise reduction from pavement as an added benefit. A typical cross section of the corduroy pattern from a diamond ground surface involves three distinct parameters, namely Height, Land Area and Groove Area as shown by Figure 16. These parameters are decided using the requirements of the project. The typical range of values for these parameters as specified by the FHWA are given in Table 3 [26] [27].

Table 3: Typical Values for diamond grinding design

Parameters	Values
Groove	2 – 3 mm
Depth	1.5 -2 mm
Number of Grooves	180 - 200 /m

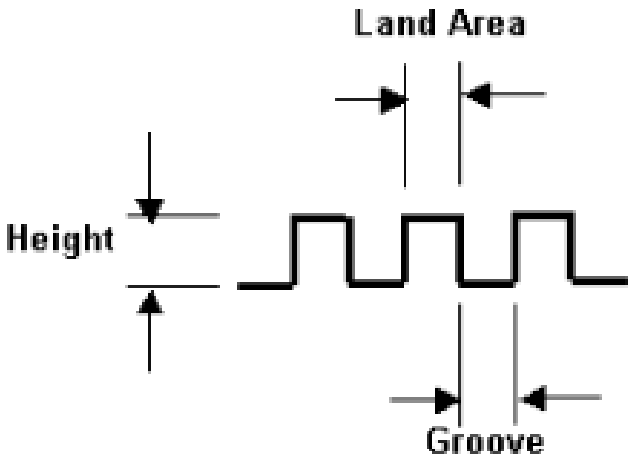

Figure 16: Grinding Surface - Lateral Cross Section

The other important parameter to be considered that affect the Land, Groove and depth is the placement of diamond cutting blades. These are decided by the parameters, specifically, the width of the cutting head and blade spacing. The typical values are provided in Table 4. The saw blades are also selected taking into consideration the diamond concentration, diamond size and bond hardness of the surface. Figure 17 shows a diamond grinding head

with pedestal bearing on the ends. This entire system is mounted on the machine and connected to a motor.

Table 4: Typical values for grinding head parameters

Parameters	Value
Cutting Head Width	900 to 1200 mm
Blade spacing	164 to 194 /m

Figure 17: Diamond Grinding Head

2.4.3 Diamond Grinding Machines

There are currently two types of grinders available commercially, they are broadly classified into Fixed Frame and Swing Frame grinders based on their construction and degrees of freedom.

2.4.3.1 Fixed Frame Grinders:

These are a single frame design with all parts including grinder head, ground wheels, water tank, fuel tanks and vacuum systems all attached to the same frame. All parts are mounted on the same frame and hence the equipment moves as on single body with no secondary frame. The PC 4500, PC 1500 and Penhall G-38 are some examples of these type of grinders.

Figure 18: PC 4500 - Single Frame Grinder

2.4.3.2 Swing Frame Grinders:

Swing Frame Grinders involve a main frame and a secondary frame with pivot points in the front, rear and in the middle connecting them together. The ground wheels and ancillary equipment such as the tanks and vacuum systems are part of the main frame while the secondary frame houses the grinding head. The pivot allows the secondary frame to swing about the main frame. The PC 6000 is an example of these type of grinders.

Figure 19: PC 6000 - Swing Frame Grinder

2.4.4 Diamond Grinding – Benefits

Diamond Grinding provides many benefits for pavement performance. [27]

- Provides a smooth riding surface with good IRI reduction.
- Improves surface texture and enhances acoustic performance.
- Enhances hydroplaning resistance due to corduroy texture.
- Increases pavement life by about 15 years on average [28] [29].
- Can be employed to correct spot roughness or miles of highways.
- Can be done with traffic flowing in other lanes.
- Low cost when compared to Asphalt overlay [30]

2.5 Grinding Simulators

Diamond Grinding process is really powerful for improvement of pavement performance. But, users also need to understand the effects of grinding at a particular setting and the level of improvement they can achieve. This is where grinding simulators such as the Smoothness Assurance Module in ProVAL© are utilized. The SAM module in ProVAL© can be utilized to perform different types of "What-ifs" analysis for grinding projects to predict IRI improvements and post grind profile. The SAM module can be used to determine out of spec locations and provide must grind recommendations. A brief overview of the SAM module is provided in the following section [11].

2.5.1 Smoothness Assurance Module

The SAM module accepts road profile in Pavement Profile Format (PPF), ERD (Engineering Research Division format of the University of Michigan Transportation Research Institute, UMTRI) or other ASCII formats acceptable to ProVAL [31], analyse the data, grind the profile at a particular setting and output grind locations and warnings. The start-up screen in the module collects inputs with respect to roughness measurement from the user as shown in Figure 20. These inputs include the elevation profile, roughness threshold limits, type of roughness measure (IRI, MRI, PRI, etc.), filtering wavelengths and wheel path

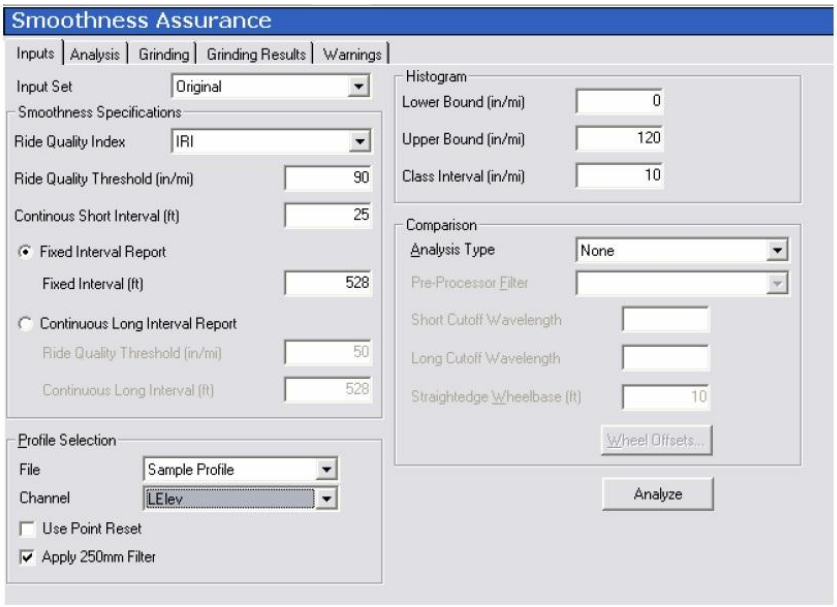

Figure 20: SAM Input Screen

The grinder screen of the software analyses the profile against thresholds and provides must grind locations with grinder settings as shown in Figure 21. Strategy management options are shown in Figure 21. Locations button can be used to select or deselect certain locations from the list before simulation. Strategy button allows user to toggle between several saved strategies to compare results. Auto-Grind provides an automated list of grind locations suggested by ProVAL©.

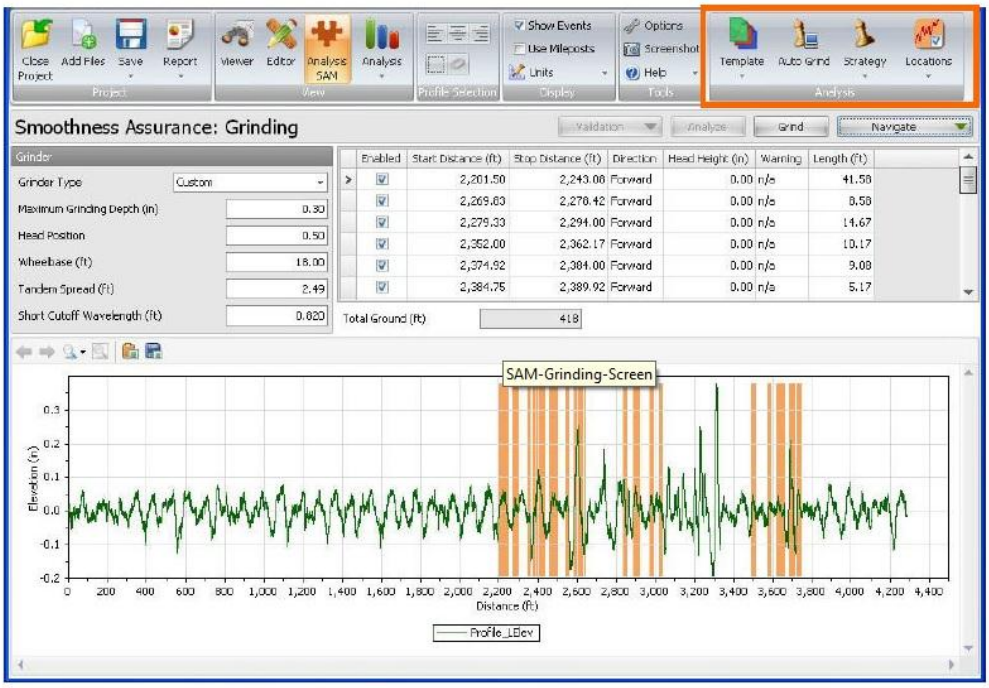

Figure 21: SAM Grind Interface

The simulator then collects grinder information including Wheelbase, Max Grind Depth, Tandem Spread and Head Position. The physical meaning of these parameters is provided in Figure 22. ProVAL© provides two inbuilt grinders (18ft wheelbase and 25ft wheelbase) as well as a custom grinder.

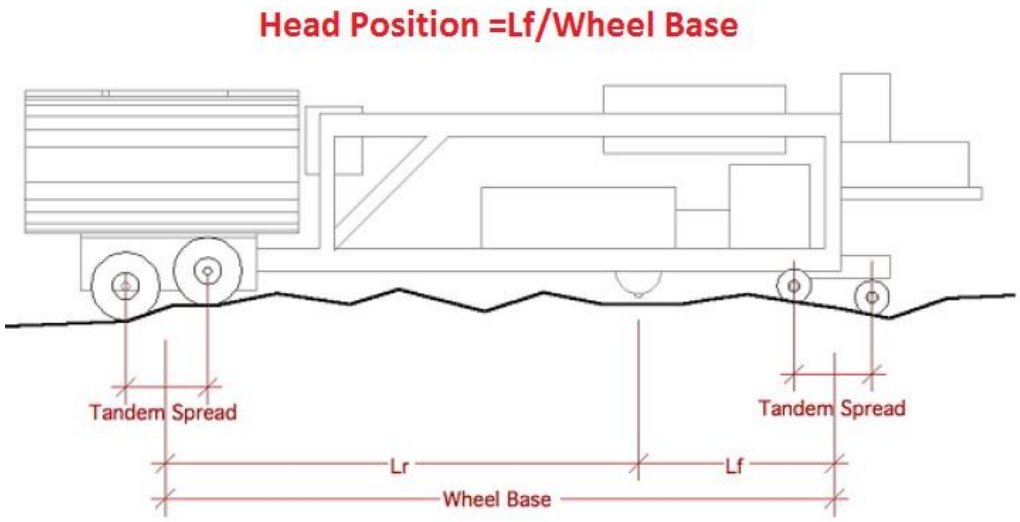

Figure 22: Grinder Schematic

The simulator results for the Auto Grind are tabulated. The user can then enable or disable grind locations thereby optimizing the grind locations and compare IRI improvements. The user can also change the Direction, Start and Stop Distance and Head Height above ground at the start of the process to obtain different post grind pavement properties. Once the user has defined the grinding strategy, the results can be documented for future use.

These commercial simulators are very useful in finalizing a grinding strategy before carrying out the process in the field, but they also need manual optimization needed to arrive at the ideal strategy. The work aims to address this issue by automating the process of grinding location selection by implementing a genetic algorithm that can go through the search space and provide the optimum strategy.

2.6 Grinding Simulation Algorithm

The Smoothness Assurance Module uses a method for predicting the post grind surface of the grinding process using the work published by Steven M Karamihas [32]. The parameters needed for grind simulations are the position of the four tandem wheels and the grinding head

longitudinally along the road surface as shown in Figure 23. The longitudinal distance is used to obtain the elevation at these locations (Elevation profiles provide elevation with respect to longitudinal distance).

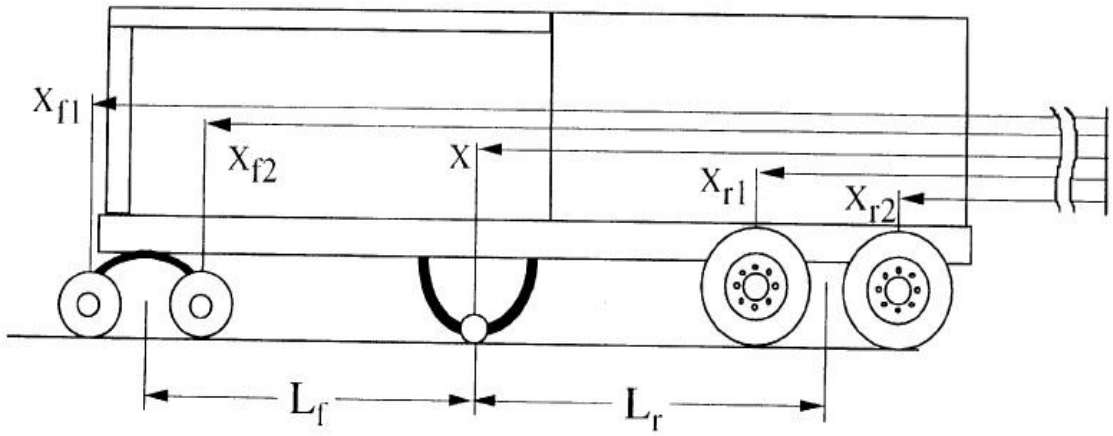

Figure 23: Grinder – Parameters

The first step in the algorithm is to identify the location of the Grinding head reference frame. The location of the grinding head reference, elevation of front tandem wheels and read tandem wheels are provided in Figure 24. This is calculated from the average elevation of the front and rear tandem wheel elevation as shown in (14), (15) & (16). $P_s(x)$ is the smoothed elevation profile at longitudinal distance x.

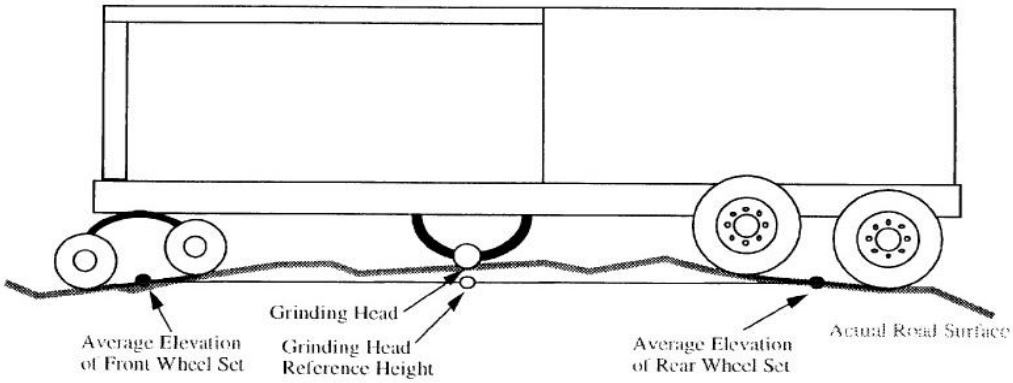

Figure 24: Grinder Reference Plane Location

$$H_f = 0.5(P_s(X + X_{f1}) + P_s(X + X_{f2})) \quad (14)$$

$$H_r = 0.5(P_s(X + X_{r1}) + P_s(X + X_{r2})) \quad (15)$$

$$H_{ref} = \frac{\left(\left(L_r . H_f\right) + \left(L_f . H_f\right)\right)}{\left(L_r + L_f\right)} \tag{16}$$

Once the grinder reference place has been located, the height of the grinding head from the ground using is calculated as (17). The head height is maintained constant and the grinder is inched forward along the profile. When the grinder head protrudes beneath the profile, grinding occurs to establish the ground profile. If the grinder does not protrude, the input profile is not altered at that location. The values of H_f& H_r are recalculated at all locations based on profile. The H_r is now calculated using the ground profile elevation rather the original (18). $G(x)$ is the ground elevation profile at longitudinal distance x. If, the rear wheels have a track wider than the grinder width, then they do not traverse the grinded profile and hence the original formula should only be used.

$$H_{head} = P(x) - H_{ref} \tag{17}$$

$$H_r = 0.5(G(X + X_{r1}) + G(X + X_{r2})) \tag{18}$$

The grinding reference place is also recalculated and then it is determined if grind takes place or not based (19) and (20). The grinder is incremented over the entire distance of the profile to identify the post grind surface. This algorithm is used in commercial grinding simulators to calculate post grind surface. But, the effect of the cut depth and speed are not considered in this work. Whereas, real grinder frames have the freedom to move up or down based on these parameters which will affect the location of H_{ref} & H_{head}.

$$P(X) \leq \left(H_{ref} + H_{head}\right), G(X) = P(X)(No\ Grind) \tag{19}$$

$$P(X) > \left(H_{ref} + H_{head}\right), G(X) = H_{ref} + H_{head}(Grind) \tag{20}$$

According to (19) and (20), the depth of material removed is exclusively based on the kinematics of the grinder with no effect due to grinder speed and depth. That is, compliance of the grinder is not modelled. The following sections of this research aims to address this by the development of a complaint grinder model that calculates ground surface from speed and cut depth.

2.7 Genetic Algorithms – An Introduction

A Genetic Algorithm methodology will be employed due to its suitability to the problem. Genetic algorithms are robust, quick and are naturally parallelizing [34]. Genetic algorithm is one of the evolutionary computation techniques that employs methods of human evolution to optimization problems. The optimization is based on a natural selection of "survival of the fittest" to arrive at the optimum solution. When compared with conventional optimization techniques such as Gradient Search methods, Genetic algorithms (GA) have the following advantages that make it perfect for the application [35].

- They naturally search a number of possible solutions (Inherent Parallelization) which is needed due to large search space that we have for the grinding simulator.
- Genetic Algorithms do not need derivatives and can operate directly on the objective function. Since grinding costs are an absolute function for which a derivative does not exist, GA's are a natural choice.

Genetic Algorithms involve the following major steps for setting up the problem and carrying out the process of identifying the global optimum

- The first step is to code the possible alternatives as a binary set of 0's and 1's. Care as to be taken to make sure that each code represents a unique solution
- The genetic algorithm them selects a set of alternatives from the search space and computes the fitness against the objective function.
- Once the fitness is calculated, three distinct GA operations namely Selection, Reproduction and Mutation take place.
- These operators are a method to select the fitter parents and create a new population of fit offspring's
- Then, the unfit parents are replaced and the new population goes through the same steps till the solution has converged.

2.7.1 Encoding the variables

The first step in the process is to encode the alternatives available in a binary set of 0's and 1's that are both unique and spans the entire search space.

2.7.2 Selection of Initial Population

The next step in the process is selecting the initial population, the size of the initial population (N) is determined from the number of bytes in the encoded variable [36]. Hence a random population of that size is selected to begin the algorithm. The fitness of each individual is computed.

2.7.3 Selection of Parents for Reproduction

The next step is to select the individuals to obtain the next generation of individuals. The selection process is carried out by a process of "Weighted Roulette Wheel" selection [35]. A weighted roulette wheels includes slots that are biased based on the fitness of the individual compared to the population fitness. Then 'N' number of individuals are selected by "spinning the wheel and selecting the individual slot that comes up".

2.7.4 Crossover - Reproduction

The next step is to produce the offspring using the crossover technique. Crossover is carried out selecting two individuals from the parent population in random and combing them using the technique of "two-point conversion". The crossover operator randomly selects a cross over site along the bit and combines the two strings as shown in Figure 25. Crossover occurs at a probability defined as Crossover Probability (P_c). Crossover probability preferably should be high to make sure that we get higher number of offspring to continue to the next step. It is usually maintained between 80% - 95% [34] [36].

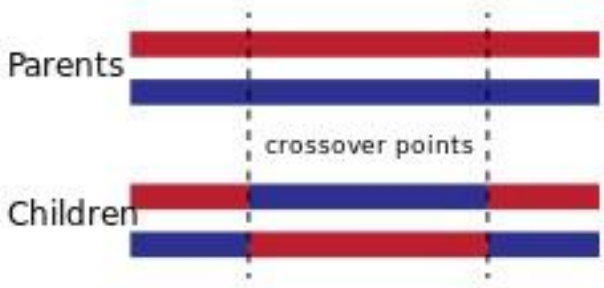

Figure 25: Two Point Crossover

2.7.5 Mutation

The other operator is the mutation operator. This operator is essential in making sure that the search algorithm does not get pulled into local maxima's over global maxima's. The mutation operator randomly selects location along an individual to flip it. (i.e. 1's to 0's and 0's to 1's). The mutation operator should not occur at a very high probability to protect the genetic search from becoming completely random. A Mutation probability (P_m) of about 0.5% to 5% is usually employed.

2.7.5.1 Replacement

The final step is the replacement of the parent population with the new offspring. This is carried out using a weak member replacement. Once two parents are combined through crossover and mutation, the offspring and parents are compared against the objective to select the fittest of the set into the next generation. Notice that the fittest can also be the parents. This will weed out weaker solutions and help in obtaining faster convergence.

2.7.5.2 Convergence Criteria

The convergence criteria for the algorithm is two part. The first part is a number of iteration constraint that forces the algorithm to cycle through a minimum number of generations before checking convergence. Once the number of generations has been satisfied, the algorithm compares the average fittest of the preceding generation against the present generation. Once it is at a point when improvement is not possible, the solution has been converged

3. Development of a Grinding Strategy Algorithm

The various aspects of developing the automated grinding strategy algorithm that is the main objective of this research project is discussed in this chapter. First a discussion on the cost optimizing function is discussed. This is followed by the development of the complaint grinder model for post grind surface prediction. Finally, an example genetic algorithm for optimizing grind locations using the cost function is laid out.

3.1 Development of an Objective Function

The first goal of this work is the development of a means to include the cost of grinding in making grind/no grind decisions that results in a grinding strategy. Specifically, the objective function should be developed such that the minimum amount of grinding possible is performed to bring the pavement into specifications. The costs generally depend on surface properties, material removed, and smoothness requirements [27]. The costs are typically classified in two broad categories.

- Material Removal Costs.
- Equipment Operating Costs.

3.1.1 Material Removal Costs

The volume of material removal addresses the need to minimize the amount of grinding that is being carried out in the project. The volume of material directly translates to expenses due to the costs in disposal. The vacuum system in the grinders sucks out the removed material in slurry form. This slurry needs to be disposed with compliance to environmental regulations. Hence the material removal costs can be expressed as (21)

$$Material\ Removal\ Costs\ (M) = k * Volume\ of\ Material\ Removel(V) \qquad (21)$$

The cost per volume parameter, k, greatly affects the grinding strategy. For example, if it's a rural project which allows slurry to be dumped along the highway, the cost per volume value will be low and more grinding will likely take place. Based on if the project is urban or rural and also surrounding conditions, it may not be permissible to simply dump the

slurry along the side of the highway, but would need to be transported to a designated dump site for disposal. This could greatly increase the volume removal costs and the cost per volume parameter need to be adjusted to reflect this reality.

3.1.2 Equipment Operating Costs

The second category is associated with operating the equipment and all the auxiliaries for performing the operation. One aspect of the objective function then, is to reduce Operation and Maintenance costs for grinding contractors. Diamond grinders have a fuel consumption from 10 gallons/hour to 30 gallons/hour. The operating costs also include assisting equipment such as water pumps and a vacuum system for slurry removal, staff and personnel and other miscellaneous expenses. This is expressed as follows.

$$Operating\ Costs\ (O) = H * Operating\ Time \tag{22}$$

Here $'H'$ is the hourly operating costs of the equipment as specified by the contractor. This will differ based on the type of project, type of equipment and personnel. Projects with hard pavement structure will have higher wear on the cutting head resulting in higher operating costs and vice versa. Hence the type of project can result in higher or lower importance for this criterion while deciding the grinding strategy.

3.1.3 Objective Function

Now that the costs have been identified, they need to be bundled them into an appropriate cost function that can then be minimized subject to performance constraints. A "Linear Absolute Objective Function" is used for this particular application due to the following reasons [33].

- The different categories discussed above are linear with respect to the amount of grinding carried out. In order words, they linearly increase with increased amount of grinding.
- The absolute function is preferred over squared since they do not place higher importance on outliers. An absolute function will place equal importance on all alternative grinding strategies.

Hence, we now define the objective function that will be minimized to achieve the optimum grinding strategy for a given project.

$$Cost\ of\ grinding\ (f(g)) = (k * V) + (H * T) \quad (23)$$

3.2 Development of grinding models:

The second objective is to achieve better post grind surface prediction through the development of compliant grinder models. Current commercial grinding simulators utilize a grinder model that does not factor cut depth and speed of operation while predicting material removal [32]. Commercially available diamond grinders are similar in construction to the grinder sketched in Figure 26. The figure shows the grinder frame which includes the grinding head which can be lowered and raised using hydraulics. These hydraulic cylinders also prevent the head from raising up when they come in contact with the surface using hydraulic pressure. The hydraulic cylinder's pressure settings is shown in Figure 27 prevent the grinding head to rise up or down due to surface interactions. That is, if reaction forces from the pavement is lower than the pressure on the head, there is no change in head height. But, on the event of a deep cut or high speed, the force from the surface may exceed the hydraulic pressure from the top causing the grinder to rise up. This effect is coined as "head riding out a cut" in the industry.

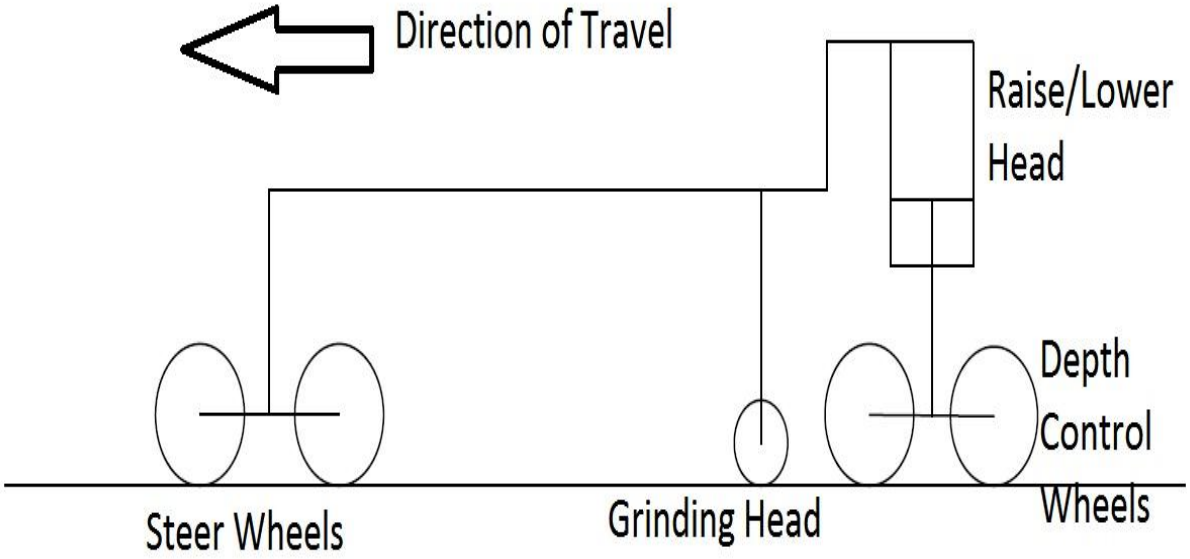

Figure 26: Generic Grinder Sketch

Figure 27: Hydraulic Pressure Setting Display

The parameters that effect grinding a particular location are shown in the sketch in Figure 28. R is the radius of cutting head, α is the angle formed by the sector of the cutting head in contact with the pavement, δ is the cut depth at that location and v is the velocity of the grinder through the cut. These parameters are used to calculate the vertical force acting on the grinder in the following section

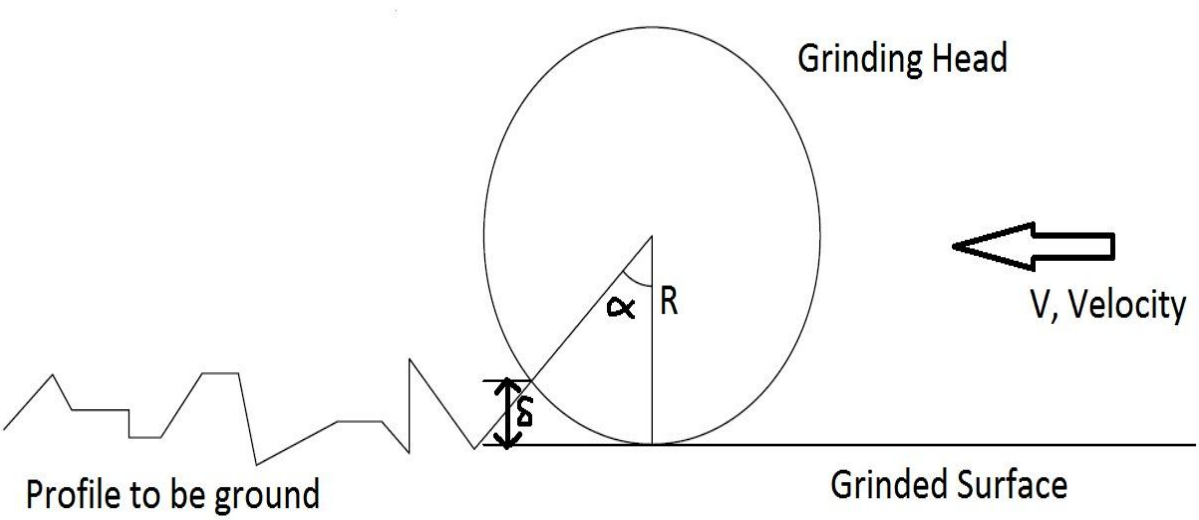

Figure 28: Grinding Operation: Schematic

3.2.1 Calculating Vertical Force on Grinder from Road Surface

Consider small increments in cutting angle with infinitesimally distance moved along the surface. The material removed during this increment can be given as follows, where $'\delta'$ is the depth of cut and $'\alpha'$ is the angle of attack. $'du'$ is the distance moved along the surface in time $'dt'$

$$dz = Rd\alpha \sin\alpha \tag{24}$$

$$dM = du.dz = du.Rd\alpha \sin\alpha \tag{25}$$

$$Rate\ of\ Material\ Removal = \frac{dM}{dt} = v.Rd\alpha \sin\alpha \tag{26}$$

Now assuming that the tangential force acting on the grinding head is directly proportional to the rate of material removed. The tangential force and its vertical component can be calculated as given below where B is a constant of proportionality.

$$F(\alpha) = B.vRd\alpha \sin\alpha \tag{27}$$

$$F_z(\alpha) = B.vRd\alpha \sin^2\alpha \tag{28}$$

The total vertical force can then be calculated at the grind location by integrating (28) over the entire angle of attack and then considering small angle approximation

$$F_z(\alpha) = BvR.\int_0^{\alpha} \sin^2\theta\, d\theta \tag{29}$$

$$F_z(\alpha) = BvR\left[\frac{1}{3}\theta^3\right] \tag{30}$$

Now, recall the geometry of the cutting operation, the angle of attack is a combination of the cutting head radius and the depth of cut. Hence substituting that into the expression for the total vertical force can be written as

$$\alpha = \sqrt{\frac{2\delta}{R}} \tag{31}$$

$$F_z(\alpha) = \frac{Bv\delta^{\frac{3}{2}}}{R^{\frac{1}{2}}} \tag{32}$$

3.2.2 Calculating Actual Cutting Depth

From (32) replace the combination of speed and cutting depth with a new variable called as $'\beta'$ Also consider a critical combination of these parameters called as $'\beta^{*}'$ which will be provided by the contractors using the algorithm. This will be a value of speed and depth that through experience is known to result in "grinder riding out a cut". The algorithm will then also calculate the actual $'\beta'$ to decide on type of grinder model to use.

$$dF_z(\theta) = \frac{B}{R^{\frac{1}{2}}}.\beta, where\ \beta = v.\delta^{\frac{3}{2}} \tag{33}$$

$$if\ \beta > \beta^{*}, \delta_{actual} = \left(\frac{\beta^{*}}{v}\right)^{\frac{2}{3}} \tag{34}$$

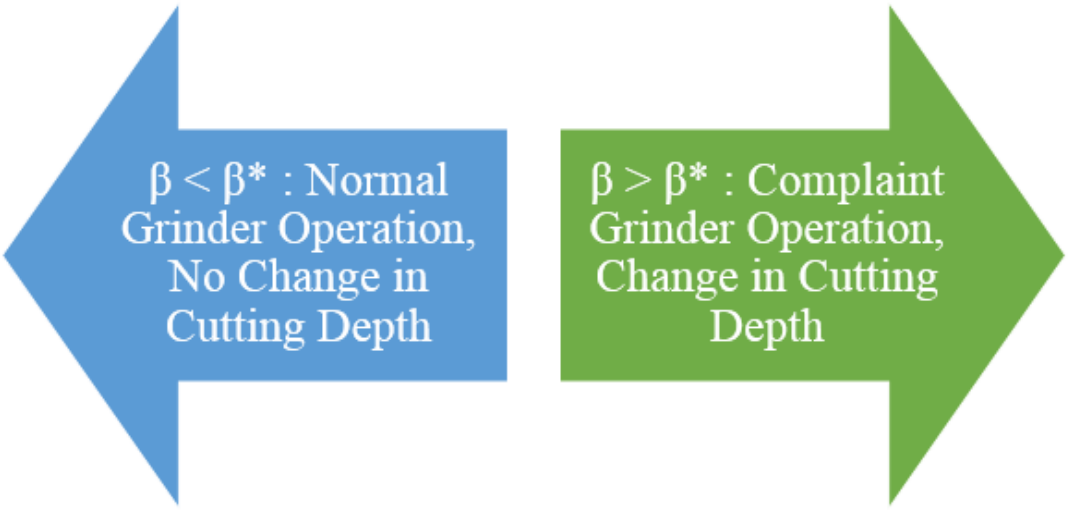

Figure 29: Selection of Grinder Models

3.3 Cost Optimization through genetic Algorithms

This section shows the use of genetic algorithms for optimizing grind locations for cost minimization. The algorithm will aim to minimize the objective function (23) with respect to performance constraints. The major parameters that decide the grinding strategy are given below. Depth and pass are the only constraints that can be modified at each location as different strategies and will be part of the encoded variable for the genetic algorithm.

1. Maximum allowable depth of grind
2. Minimum increment in depth of grind
3. Minimum length of a grind locations
4. Minimum length between grind locations
5. Number of passes

Initially, the road surface is converted to a roughness profile and locations of high roughness are identified as grind locations. Following that, grind locations are combined based on minimum length of grind and minimum distance between grinds. Now consider a road surface as the one shown in Figure 30. Assume based on constraints, section 1 and 4 are grind locations. Following this, parameters in Table 5 are used to encode the genetic algorithm is carried out as shown in the following sections

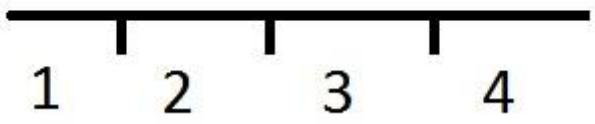

Figure 30: Example Surface discretized into segments

The number of distinct depth and pass alternatives are calculated as shown in (35) and (36), using which the number of bytes for each is calculated (37) and (38). This is then used to calculate the total number of bytes for each alternative and also the size of the initial population for the genetic algorithm. Following this, they are encoded in a binary set of 1's and 0's from 0 to number of alternatives. That is 0 means 0 cut depth, 1 means 0.1 cut depth and so on. Table 6 shows the coded variables and there decoded values of depth and pass for this example.

Table 5: Genetic Algorithm Example Parameters

Parameter	**Value**
Maximum depth of cut	0.3 in
Depth of cut increment	0.1 in
Minimum number of passes	1
Maximum number of passes	1

$$depth\ alterative = \frac{0.3}{0.1} + 1 = 4 \tag{36}$$

$$pass\ alternatives = pass_{maximum} - pass_{minimum} + 1 = 1 \tag{36}$$

$$depth\ bytes = \frac{\log alternatives}{\log 2} = \frac{\log 4}{\log 2} = 2 \tag{36}$$

$$pass\ bytes = 1 \tag{38}$$

Table 6: Encoded and Decoded Variables

Coded Variable	Decoded Depth	Decoded Pass
000	0	1
010	0.1	1

100	0.2	1
110	0.3	1

The alternatives are combined for each grinding location, for example, the considered road has two grind locations. Hence ′000110′ will be one of the alternatives where the first three bytes are depth and pass for location 1 and last three bytes are depth and pass for location 4. From this sample space, an initial population is selected to start the genetic algorithm. The initial population is decoded and grinding operation is simulated for each alternative. The cost for each alternative is calculated and its percentage against the cost for the entire set is also calculate as shown in Table 7. All values in the example are for understanding purpose and don't reflect a real operation

Table 7: Cost and Percentage Cost

Initial Population	Cost	Percentage Cost
000010	$45	45%
010110	$20	20%
100000	$35	35%

The percentage cost values are used to select the parents for the generation on a process called Weighted Roulette wheel selection. A roulette wheel is biased as per the percentage cost (that is lower cost alternative have higher probability of turning up when the wheel is spun). The wheel is then spun three times to select three individuals for reproduction. Note, that an individual can even be selected twice based on the wheel. This second generation undergone a process a reproduction and mutation as explained in chapter 2 to produce children. The process is repeated to produce more generations till the convergence criteria is reached. The lowest cost alternative of the final generation is then outputted to the user.

4. Results & Discussions

4.1 Results of grinding simulator

4.1.1 Comparison with ProVAL on post grind surface prediction

The first step in testing the Grinding Simulator is to compare it with the industry standard – Profile Valuation and Analysis (ProVAL©). ProVAL© allows its users to carry out grinding simulations as part of its Smoothness Assurance Module (SAM). Comparisons between the results from the SAM module and VTPL's simulator for different test sections are carried out to assess the improvements in cost and performance using the proposed method. Six different datasets collected from actual highways in the United States were used for testing the simulator. Table 8 shows the properties of these data sets and any special characteristics for choosing the same.

Table 8: Sample datasets for testing

S. No	Length of Profile (ft)	Characteristics
1	14528.50	Smooth road with one high bump which will cause increase in Beta value
2	84674.75	Long Profile to test algorithm running time
3	7401.92	Profile with high number of short violations that will be difficult to grind out
4	4870	Smooth road with one location of non-compliance to roughness specification
5	3487.50	PCC pavement with a high number of localized roughness events
6	1111.83	Short profile with both long and short violations

4.1.1.1 Comparison of 100% grind over the entire surface.

First consider a comparison between the two simulators while performing 100% grind operations (i.e. grinding the entire length of the profile with the grinding head flush against the road profile at the start location). These are called Blanket Grind operations where the

entire profile is ground on old pavements to improve surface texture properties. The following graphs show a comparison between the simulators. Figure 31 and Figure 32 show the difference between amount of material ground in ProVAL© and VTPL's simulator as well as the "beta value" from the VTPL simulator for dataset 1. One of the objective of the work was to develop a grinding simulator that produces post grind surface prediction similar to the industry standard (ProVAL©) while including effect of speed and cut depth. Figure 31 shows that difference between amount of material ground is almost zero except of the location of high "beta value" where the ProVAL over predicts material removed since it has not factored the head riding out the cut. Figure 32 shows the same operation simulated with a higher beta star value. This shows that by increasing the beta start value, the compliance in the grinder can be reduced and the results become similar to ProVAL (i.e. Due to the high beta star value, the grinder never transitions into the compliant grinder mode)

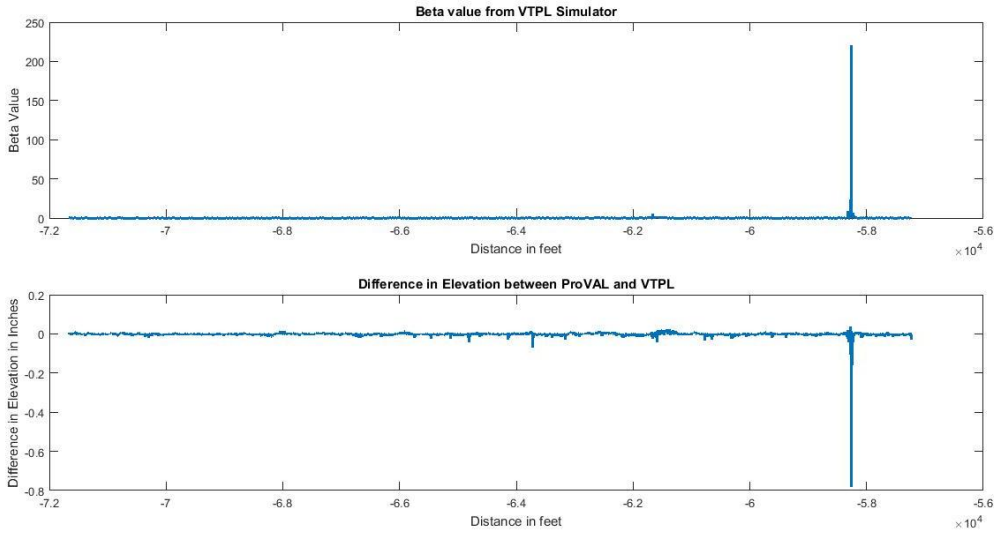

Figure 31: Comparison between ProVAL and VTPL with beta star = 60

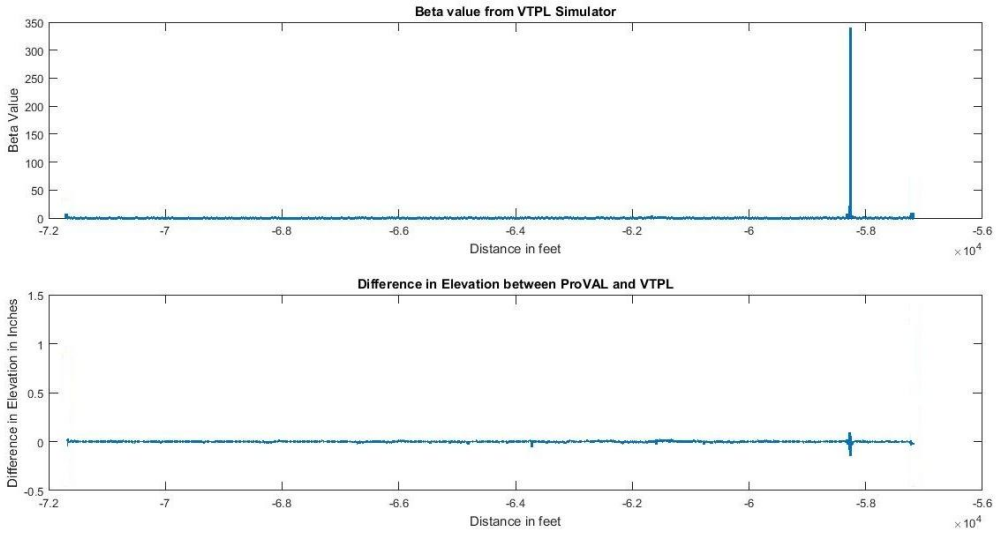

Figure 32: Comparison between ProVAL and VTPL with beta star = 5000

4.1.1.2 Comparison using Spot Grind Application

Following the single grind (Blanket grind) comparison, spot grind comparison between the two elevation profiles was carried out. Spot grinding is more representative of an IRI correction project, where users only grind locations of higher roughness. From Figure 33 and Figure 34, grinding has only taken place in the three or four distinct locations which were provided to the program. Also, the average difference between the two profiles is 1/10 of an inch which proves good conformance between the two simulators. Furthermore, considerable differences occur between the two profiles only when the "Beta value" increases which also confirms to the developed grinder model and the goal of developing complaint grinders in simulations.

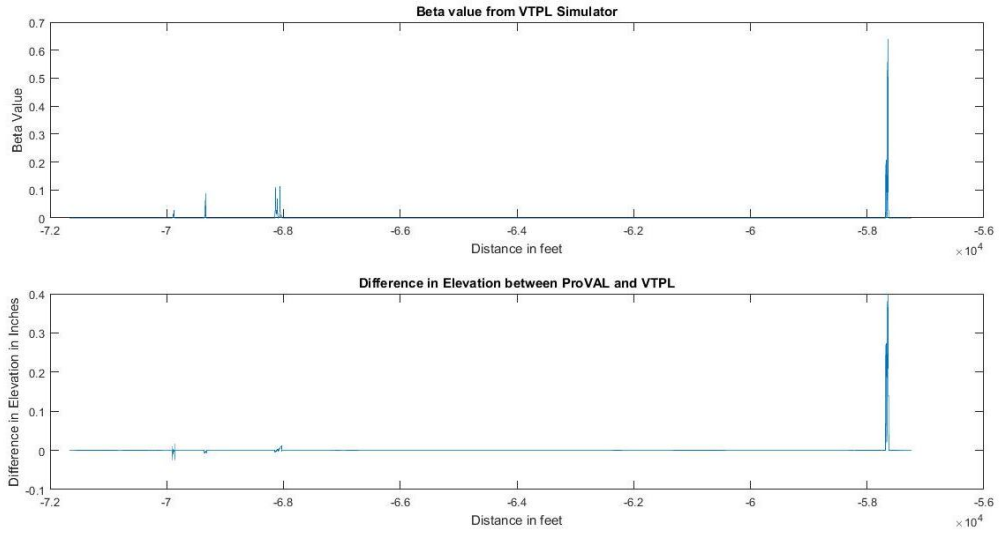

Figure 33: Beta Value and difference Plot –Dataset 1- Spot Grinding

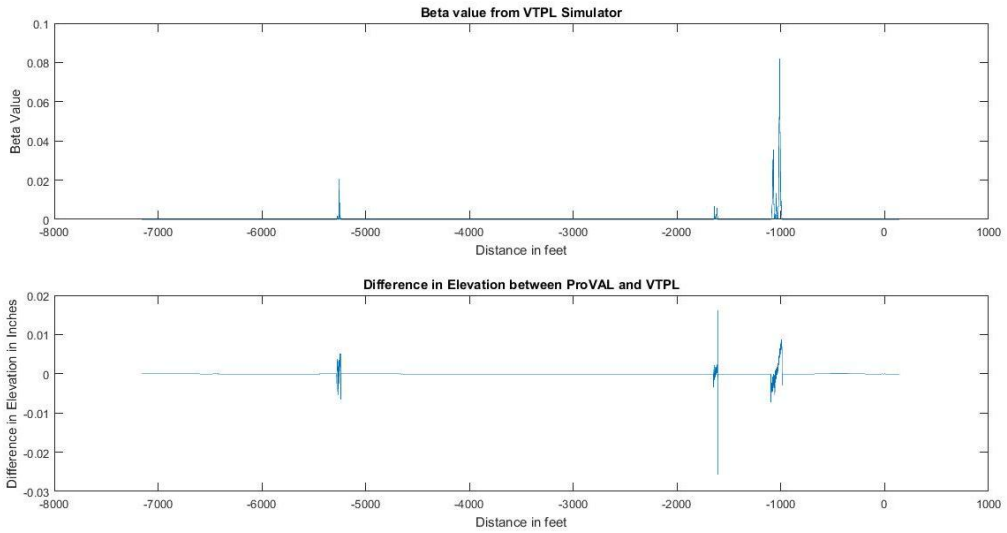

Figure 34: Beta Value and Difference Plot - Dataset3 - Spot Grinding

4.1.2 Comparison of cost benefits against "Auto-Grind"

The effectiveness of the optimization algorithm was compared against ProVAL's© "Auto-Grind" feature which provides must grind locations bases on roughness specifications. The results are herewith provided. The IRI specifications used for the comparison are provided in the Table 9.

Table 9: IRI Specifications for comparison and parameters

Description	Specification
Short Continuous IRI	160 in/mi
Long Continuous IRI	90 in/mi
Cost of material	$700 /cum
Cost of equipment	$1200 /hr

The original profile was grinded as per the grinding locations provided by both the programs. The grinded profile was then used to identify amount of volume removed and also the time the grinder would be used in each scenario. Table 10 shows the comparison over equipment costs over three datasets. Table 11 shows the comparison over material removal costs while Table 12 shows the comparison in terms of number of IRI violations. Now consider dataset 2, ProVAL's© "auto-grind" results in 6 Short IRI violations with a grinding strategy that will cost a total of $ 4931.84 while VTPL's simulator also results in 6 short IRI violations but with only a total cost of $ 1262.41. Costs benefits are also apparent in datasets 1 and 3 even though there is an increase in number of violations. The user can then use their knowledge of specific projects to relax or tighten constraints to obtain different strategies before making a decision. For example, certain projects allow certain number of violations without any penalties while other might require complete removal of non-conformance before completion.

Table 10: Equipment Running Costs

Dataset	ProVAL	VTPL
4	$ 83.33	$ 57.7
3	$ 478.24	$ 255.21
6	$ 651.17	$ 505.47

Table 11: Cost of Material Removal

Dataset	ProVAL	VTPL
4	$ 1044.5	$ 258.82
3	$ 4453.6	$ 1007.2
6	$ 8745.2	$ 3038.4

Table 12: Comparison of IRI Violations

Dataset	ProVAL	VTPL
4	No Violations	1 Short Violation
3	6 Short Violations	6 Short Violations
6	4 Short Violations 3 Long Violations	5 Short Violations 4 Long Violations

4.2 Discussions

4.2.1 Comparison of the grind locations – Feasibility of grind locations

Table 13 shows a list of grind locations provided by "Auto-Grind" feature in ProVAL. The highlighted cells show some of the drawbacks that formed the motivation for this work. These suggested grind locations are very closely placed to each other, that the user will need to manually combine them for the final grinding strategy. Table 14 provides the grind locations provided by VTPL's grinding simulator for the same dataset. These grind locations are controlled by the constraints set by the user and hence are automatically optimized to combine closely placed locations into a single location. Thereby engineers using the VTPL simulator will not need to manually optimize locations thereby saving time in developing grind strategies.

Table 13: Auto - Grind Locations provided by ProVAL

Start Distance (ft)	Stop Distance (ft)	Distance Between Grinds (ft)	Length (ft)
-7197.083	-7144.917	3202.417	52.17
-3942.5	-3926.5	36.333	16
-3890.167	-3847.083	17.75	43.08
-3829.333	-3814.583	0.416	14.75
-3814.167	-3805.333	23.416	8.83
-3781.917	-3753.333	1635.083	28.58
-2118.25	-2097.666	10.25	20.58
-2087.416	-2079.5	8.584	7.92
-2070.916	-2052.916	1.916	18
-2051	-1998.916	0.666	52.08
-1998.25	-1972.666	47.25	25.58
-1925.416	-1805.166	527.583	120.25
-1277.583	-1234.333	57.25	43.25
-1177.083	-1160.416	28.25	16.67
-1132.166	-1121.666	-	10.5

Table 14: Grind Locations - VTPL Simulator

Start Distance (ft)	Stop Distance (ft)	Distance Between Grinds (ft)	Length (ft)
-4091	-4082	269.7	9
-3812.3	-3769	1488.1	43.3
-2280.9	-2270.2	304.7	10.7
-1965.5	-1908	99.4	57.5
-1808.6	-1784	628.3	24.6
-1155.7	-1103.1	160.02	52.6
-943.08	-918.08	334.16	25
-583.92	-557.08	275.33	26.84
-281.75	-276.08	276.08	5.67

4.2.2 Identifying Grind Locations

The next challenge is in identifying the grind locations that are out of specification automatically. The comparison between ProVAL and VTPL's simulator can be explained

using this sample dataset. Figure 35 shows the pre-grind Short continuous IRI of the right wheel path. The plot shows that the road profile has only one region which is out of specification between 3800 ft to 3500 ft.

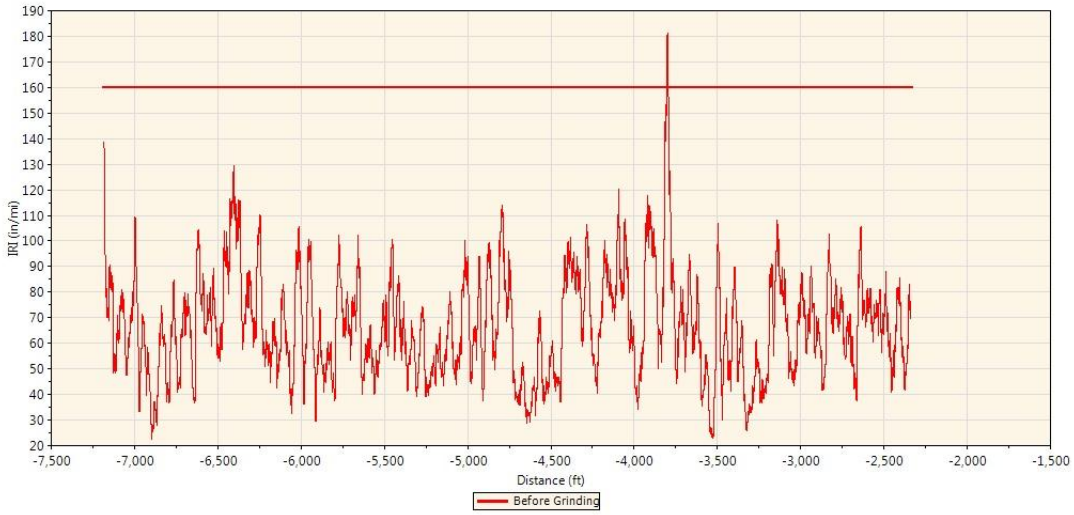

Figure 35: Pre-Grind Short Continuous IRI

Table 15 and Table 16 shows grind locations suggested by ProVAL and VTPL's simulator. The ProVAL auto grind engine has provided five locations with two locations that will be combined by an engineer due to feasibility issues. Whereas the VTPL simulator has provided a single grind locations of 142 feet. Both programs have provided locations along the same locations but the VTPL simulator has also optimized these into single a long grind which will be easy to perform in the field when opposed to ProVAL's five locations. This highlights that VTPL's simulator can identify out of specifications locations similar to ProVAL with the added advantage of combining locations thereby removing the need for manual optimization by an engineer before decided on a strategy.

Table 15: Grind Locations - ProVAL

Start Distance (ft)	Stop Distance (ft)	Between Grind (ft)	Length (ft)
-3937.083	-3928.667	0.334	8.42
-3928.333	-3910.5	22.583	17.83
-3887.917	-3853.583	22.666	34.33
-3830.917	-3816.917	0.334	14
-3816.583	-3807.833		8.75

Table 16: Grind Locations - VTPL

Start Distance (ft)	Stop Distance (ft)	Between Grind (ft)	Length (ft)
-3811.9	-3954.2	-	142.7

4.3 Conclusions

The work carried out in this thesis provides a computer simulation program that predicts post grind road profile and identify must grind locations as per provided constraints. The program allows the user to develop grinding strategies based on a linear cost function that aims to minimize the total amount of grinding. The work also involves the use of compliant grinder model that will allow users to better predict post grind elevation in the case of heavy cuts or high speed operation. The "beta-value" is used to predict when the grinder goes to compliant mode. This function can be dialed up or down by the user to increase the level of compliance in the grinder. The genetic algorithm based optimization code will allow engineers to have a "one-click" solution to developing grinding strategies. The engineer can then either relax the constraints or tighten them to obtain different strategies to compare. This program will allow contractors and pavement specialists to better access grinding projects and reduce unwanted grinding of pavements.

5. Conclusions

5.1 Summary of research

From this work, a computer program for grinding simulation was developed. The grinding simulator provides a cost function based optimization code for identifying grind locations that will reduce pavement roughness while carrying out the least amount of grinding. This is achieved by the development of a genetic algorithm based optimization function that will cycle through different grind strategies and provide the user with the best possible strategy while satisfying constraints. The work also yielded the development of a complaint grinder model that mimics the motion of the grinding head during a deep cut or high speed operation. This model will assist engineers in predicting post grind elevation profile effectively. The compliance in the grinder can be tweaked by utilizing the "beta-value" function, thereby allowing them to control how much the grinder will deflect due to road loads. The simulator will aide engineers in making better informed decisions regarding grind locations and strategies.

5.2 Main Contributions

The work carried out developed a computer simulation program that predicts post grind road profile and identify must grind locations as per provided constraints. The main contributions of this work are:

- A grinding simulator to run "what-if" analyses prior to diamond grinding on actual pavements including a cost optimization function.
- Genetic Algorithm based optimization code to run through different strategies and provide the most cost effective strategy.
- Compliant grinder model that includes the speed of operation and depth of cut to calculate amount of material removed.

5.3 Future Work

5.3.1 Develop a Dynamic grinder model (PC 6000)

In the immediate future, an effort to study the multiple articulation grinders such as the PC 6000 should be carried out and incorporated into the grinding simulator. The PC 6000 grinders are made of two separate frames viz the main frame which houses the motor and auxiliary equipment while the secondary frame contains the grinding head as shown in Figure 36. The schematic clearly shows that the swing frame has two points of articulation about the main frame which can be raised high or low using the hydraulic cylinders. This multiple articulation causes them to behave differently to regular grinders like the one described in this work. A dynamic model should be developed that accounts for these multiple articulations and incorporated into the simulator thereby making it compatible to all commercial available grinder models.

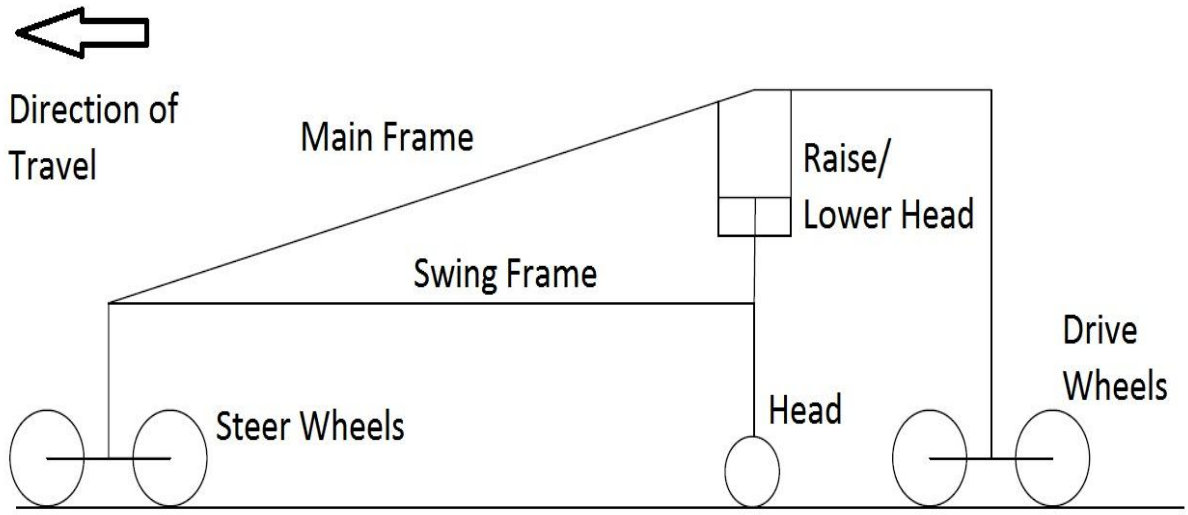

Figure 36: PC 6000 Grinder - Schematic

References

[1] S. Islam and W. Buttlar G, "Effect of Pavement Roughness on User Costs," *Transportation Research Board ,* no. 2285, pp. 47-55, 2012.

[2] American Association of State Highway and Transportation Officials, Rough Roads Ahead - Fix Them Now or Pay for it Later, Road Information Program, 2009.

[3] D. T. Hartgen, G. Fields and B. Feigenbaum, 21st Annual Report on the Performance of State Highway System, Reason Foundation, 2014.

[4] M. W. Sayers, "Profiles of Roughness," *Transporation Research Board,* pp. 106-111, 1990.

[5] I. Zaabar and K. Chatti, "Identification of Localized Roughness Features and Their Impact on Vehicle Durability," in *International Heavy Vehicle Symposium: Balancing Competing Needs in Heavy Vehicle Transport Technology*, 2010.

[6] International Grinding and Grooving Association, "CPR for City Streets," [Online]. Available: http://www.igga.net/resources/fact-sheets.

[7] R. Fung and T. Smith, "Concrete Pavement Rehabiliation Techniques and Canadian based Case Studies," in *Annual Conference of the Transporation Association of Canada*, Halifax, 2010.

[8] T. Smith, "Concrete Pavement Restoration: "Windows of Opportunity"," in *MIT Workshop*, 2007.

[9] P. Buddhavarapu, A. De Fortier Smith, A. Banerjee, M. Trevino and J. A Prozzi, "Evaluation of the Benefits of Diamond Grinding of a continously Reinforced Concrete Pavement," *Transporation Research Board,* no. 2369, pp. 59-67, 2013.

[10] B. L. Schleppi, "FHWA ProVAL Software IRI Smoothness Acceptance Analysis – Diamond Grinding Simulation," in *Proposal Note 555, ODOT Office of Technical Services*, 2014.

[11] The Transtec Group, "Smoothness Assurance Module, Field User's Manual," The Transtec Group, 2006.

[12] M. W. Sayers and S. M. Karamihas, Little Book of Profiling, The Regent of the University of Michigan, 1998.

[13] H. Chemistruck M, D. R. Zachary, J. B. Ferris, A. A. Reid and D. J. Gorsich, "Review of Current Developments in Terrain Characterization and Modelling," in *SPIE Defense, Security and Sensing*, 2009.

[14] E. Alvarez, "A Discrete Roughness Index for Longitudinal Road Profiles (Master's Thesis)," Virginia Tech, Blacksburg, 2015.

[15] M. W. Sayers, T. D. Gillespie and C. Queiroz, "International Experiment to Establish Correlations and Standard Calibration Methods for Road Roughness Measurements," *World Bank Technical Paper 45,* p. 464, 1986.

[16] ASTM Standard E1926-08, "Standard Practice for Computing International Roughness Index of Roads from Longitudinal Profile Measurements," *ASTM International,* 2005.

[17] M. W. Sayers, "On the Calculation of International Roughness Index from Longitudinal Road Profile," *Transportation Research Record,* pp. 1-12, 1995.

[18] M. W. Sayers, "Development, Implementation, and Application of the Reference Quarter-Car Simulation," in *Measuring road roughness and its effects on user cost and comfort* , ASTM, 1985, pp. 25-47.

[19] G. J. Howe, J. P. Chrstos, W. R. Allen, T. T. Myers, D. Lee, C. Liang, D. Gorsich and A. Reid, "Quarter car model stress analysis for terrain/road profile ratings," *International Journal of Vehicle Design,* vol. 36, no. 2-3, 2004.

[20] Minnesota Ashpalt Pavement Association, "Pavement Rehabilitation," in *Asphalt Paving Design Guide*, Minnesota Ashpalt Pavement Association.

[21] S. D. Tayabji, J. L. Brown, J. W. Mack, T. M. Hearne Jr, J. Anderson, S. Murrell and A. S. Noureldin, "Pavement Rehabilitation," *TRB Committee on Pavement Rehabilitation, TRB Millennium Paper Series,* 2000.

[22] "LOT Management," [Online]. Available: http://www.lotmanagement.com/asphalt-overlay-patch-or-replace/?c=lot-management-news. [Accessed 11 November 2016].

[23] American Association of State Highway and Transporation Officials, "Report on Cold Recycling of Asphalt Pavements," AASHTO-AGC-ARTBA Joint Committee Task Force Report 38, Washington DC, 1998.

[24] T. T. Trussell, "Diamond Grinding of Concrete," *Concrete Construction,* vol. 31, no. 11, p. 952, 1986.

[25] C. W. Hatcher, "Concrete Bump Cutter". United States of America Patent 3037755, 5 June 1962.

[26] CALTRANS Division of Maintenance, "Diamond Grinding and Grooving," in *MTAG Volume II - Rigid Pavement Preservation*, CALTRANS Division of Maintenance, 2007.

[27] A. L. Correa and B. Wong, "Concrete Pavement Rehabilitation - Guide for Diamond Grinding," Federal Highway Administration, Atlanta, 2001.

[28] CALTRANS, "The effectiveness of Diamond Grinding Concrete Pavements in California," CALTRANS, 2005.

[29] S. Rao, T. H. Yu and M. I. Darter, "The Longevity and Performance of Diamond-Ground Pavements," The Portland Cement Association, R&D Bulletin RD118, 1999.

[30] Georgia Department of Transporation, "Georgia's Low Cost Approach to Rehabilitating Concrete Pavements," *Civil Engineering - ASCE,* vol. 53, no. 8, pp. 50-54, 1983.

[31] The Transtec Group, "ProVAL User's Guide," The Transtec Group, Austin, 2001-2015.

[32] S. M. Karamihas, "Method for Correcting the Roughness of Pavement". United States of America Patent 6682261, 27 January 2004.

[33] P. P. Ross, Taguchi Techniques for Quality Engineering: Loss Functions, Orthogonal Experiments, Parameter and Tolerance Design, New York: McGraw-HIll, 1988.

[34] D. E. Goldberg, Genetic algorithms in search, optimization, and machine learning, Reading: Addison-Wesley Pub Co, 1989.

[35] S. N. Sivanandam and S. N. Deepa, Introduction to Genetic Algorithms, Springer, 2008.

[36] "Introduction to Genetic Algorithms," [Online]. Available: http://www.obitko.com/tutorials/genetic-algorithms/recommendations.php. [Accessed 26 11 2016].